1958

Kinetics of adsorption at the solution-air interface

Terry Charles Wallace
Iowa State College

KINETICS OF ADSORPTION AT THE SOLUTION-AIR INTERFACE

by

Terry Charles Wallace

A Dissertation Submitted to the
Graduate Faculty in Partial Fulfillment of
The Requirements for the Degree of
DOCTOR OF PHILOSOPHY

Major Subject: Physical Chemistry

Approved:

Signature was redacted for privacy.

In Charge of Major Work

Signature was redacted for privacy.

Head of Major Department

Signature was redacted for privacy.

Dean of Graduate College

Iowa State College
Ames, Iowa
1958

TABLE OF CONTENTS

I. INTRODUCTION

When a fresh liquid surface is created the physical structure and constitution of the surface is, in principle, similar to that of the bulk phase, but differs specifically on a molecular scale in that the molecules at the freshly created surface now have fewer neighbors. One or more of the following processes will probably occur to lower the free energy of the surface: reorientation of surface molecules, transport of surface active solute molecules from the bulk to the surface, or transport of surface active molecules in the external phase to the surface. An experimentally measurable quantity capable of showing this change in the structure or constitution of the surface is the dynamic surface tension. The term, dynamic surface tension, is to be contrasted with the term static or equilibrium surface tension which refers to a surface that has ceased to change with time.

All three of the above processes have as yet to be completely investigated, much less understood. For example, the question of whether a freshly generated water surface reorients in a measurable time (i.e., has a measurable relaxation time) or instantaneously is unanswered. There is some evidence (11, 44) which suggests that there is a finite relaxation time, but it is based upon experiments which suffer from lack of rigorous theoretical treatment and questionable experimental techniques. It would be of value to study the effect with a method free of the above objections.

By far the most interesting of these three processes, in the author's opinion, is the mechanism by which the surface active solute molecules are transported from the bulk to the surface. It is generally thought that the controlling step is the diffusion (8, 41) from the bulk to the region immediately below the surface (subsurface). This mechanism seems incorrect, at least, when the heat of adsorption is greater than 3-4 K cal., as this is the energy of activation needed (21) for a diffusion process in aqueous solutions. The other proposal is that the actual entry into the surface is the rate controlling step, (i.e., there is an energy barrier to entry) (52, 36). Again it would be of interest to study this problem over a much wider range of compounds and distinguish between the two proposals.

The third process, by contamination of the surface, interferes in the accurate determination of the surface tension of high surface energy elements such as mercury and the molten alkali metals and does so in a very short time (i.e., .1 sec.). It would be beneficial to develop a method whereby the surface tension of the liquid metal could be measured accurately without fear of contamination.

To study the problems associated with the formation of fresh liquid surfaces a technique is needed whereby an accurate time can be assigned to each increment of the surface as it ages. Of the various methods available (33), the vibrating jet produced by an elliptical orifice appears to be the best. This technique may be used to study surfaces which are from

.005 seconds to .050 seconds old. The main disadvantage of the method is that little work has been done with the problem of the nonlinearity of the surface age as a function of the distance from the orifice and none on the effect of the non-uniform velocity profile on the jet wave length, from which the dynamic surface tension must be calculated.

The objectives of this study were as follows:

(1) Further verify the recently derived theoretical development for the effect of non-uniform velocity profiles on the surface tension in the vibrating jet method by Hansen, Purchase, Wallace and Woody (25).

(2) Show that the data for surface tension as a function of the time found by this refined vibrating jet method is not dependent upon the orifice used.

(3) Apply the vibrating jet method thus modified to establish the time and concentration dependence of the surface tension of aqueous solution of simple aliphatic compounds.

(4) Establish the kinetic mechanism of adsorption of these simple aliphatic compounds at the water-air interface.

II. LITERATURE SURVEY

A. Vibrating Jet Method

Most of the common methods (31) that have been used to study static surface tensions have been adapted to obtain data on the time and concentration dependence of the surface tensions of aqueous solutions. The limitation to all of these methods is that the dependence of surface tension on time (especially at small times) is not known accurately because of mechanics of the experiment or a lack of theory or both. Purchase (38) has given a thorough survey of the various methods attempted and their limitations.

The first mathematically rigorous treatment of a vibrating jet of a pure liquid issuing from a non-circular orifice was given by Lord Rayleigh (40). The experimental technique and theory were furthered by Pedersen (34), Bohr (6), and Stocker (48). Apparently the method was applied for the first time to determine dynamic surface tensions of aqueous solutions by Bond and Puls (8). Following this the method was used in various forms by Addison (1, 2, 3, 4) and Burcik and coworkers (12, 13, 14, 15) for further time dependence studies.

The first serious attempt to define the limitations of the vibrating jet method for the study of the time dependence of the surface tension of aqueous solutions was made by Rideal and Sutherland (41) and Sutherland (49). The theoretical

development of Bohr was the formulation usually used to compute the surface tension from the experimentally measured quantities. Sutherland (50, p. 321) summarized the assumptions in Bohr's derivation and thus the conditions that have to be met if the calculations are to be valid, as the following:

(1) The fluid must be in laminar flow.

(2) All initial disturbances caused by ejection of liquid from the orifice are absent in that portion of the jet that is measured.

(3) The vibrational components of velocity of the jet are sufficiently small that second and higher order terms are negligible.

(4) The viscosity at the surface of the jet is the same as that in the interior of the jet.

(5) The diameter of the jet is small compared with the wave length of the vibration.

(6) The effect of amplitude on the frequency is independent of the viscous forces.

(7) The only effect of the surrounding medium is its inertia.

The first condition is satisfied when the Reynolds number R ($R = \frac{\rho v r}{\mu}$, where v is mean velocity in the orifice, r is the radius of the orifice, ρ is the density of the liquid flowing through the orifice and μ is its viscosity) is less than 2,000. In the region of 2,000 the flow in the orifice becomes turbulent and consequently the jet is turbulent and breaks up

a small distance from the orifice. In the present work it was found that the best results were obtained for $R \leq 1700$.

The second condition can be met by measuring those wave lengths at a large distance from the orifice. When a time dependence study of the surface tension is being made it is essential that the wave lengths nearest to the orifice be measured. It is generally in this region that the time dependence is most pronounced. There are two causes for initial disturbance in the jet. The first is mechanical in nature (i.e., vibration, irregularities in orifice and design of the orifice) and with enough persistance this can be overcome. The second cause is due to the non-constant velocity profile in the jet caused by the orifice. The second effect was first treated by Hansen, Purchase, Wallace, and Woody (25) and will be discussed in more detail later. The non-constant velocity profile also causes the surface age to be different from that found by dividing the distance of the surface from the orifice by the mean velocity.

The fourth condition is met with pure liquids, but when the method is applied to the dependence of surface tension on time, the adsorbate molecules that enter the surface may cause the superficial viscosity to be greater than the bulk viscosity because of their lateral interaction. Rideal and Sutherland (41) believe they have evidence that the superficial viscosity is 50 per cent larger than that of the bulk for heptanol-1 solutions. However, correction for the superficial viscosity

is fairly insignificant (ca. .05 per cent) as shown by their calculations.

The fifth condition depends on the degree of approximation used in transforming Bohr's equation into a usable form and is not critical. The third, sixth, and seventh conditions are easily met in studies of either pure liquid or time dependences of aqueous solutions.

Sutherland concludes that jets may be produced which satisfy all the criteria known for satisfactory use, but which record the surface tension as being very much lower than the accepted value (i.e., 4 per cent) and hence the only condition for choice of an orifice is that the jet it produces gives the "right" answer. This attitude seems unduly pessimistic and causes one to wonder if all conditions have been correctly considered.

Rideal and Sutherland (41) have made a careful study of the variation of the surface tension of solutions with time. They were the first to make an effort to correct for difference in surface age from that calculated by dividing the distance of the surface from the orifice by the mean velocity. It is apparent that this difference is caused by the following. When the fluid is flowing in the orifice, that part of the fluid in contact with the walls of the orifice has essentially a zero velocity. The viscous drag of this layer on the next inner layer causes it to be retarded and so on into the center of the liquid. This drag imparts a velocity profile on the

liquid in the orifice. The profile is essentially constant for an infinitely short orifice and is parabolic for an infinitely long orifice. Thus when the jet issues from the orifice the velocity of the surface at the orifice is near zero and increases as a function of distance from the orifice until it is the same as the mean velocity of the jet.

Rideal and Sutherland purport to solve this problem for an analog system. They considered the orifice and jet as an infinitely thin flat plate with liquid flowing by the plate. The plate is equivalent to the wall of the inner diameter of the orifice (no slip and hence a boundary layer) and the center of the wake is equivalent to the surface of the free jet for there is no velocity component across the surface and no external retarding force on it. With these assumptions it was possible to use the solution Goldstein (22, 23) had given for this problem and his tables for numerical calculations.

The components of velocity in the center of the wake will correspond to the surface velocity. Goldstein's equation for this case reduces to

$$\frac{u}{u_o} = 1 - A\eta^{-\frac{1}{2}} - \frac{2\eta}{A^2}$$

where $\eta = x/4l$, l is the length of the plate, x is the distance measured from a point forward of the rear edge, A is a constant equal to .18733 and u_o the velocity of the undisturbed flow. Thus the age of the surface of the jet at a

distance z from the orifice is $\int_{x_1}^{z} \frac{dx}{u}$ where x_1 is such that $\frac{u}{u_o} = 0$. Then from the theory of Schiller (43) they obtained the degree to which the velocity profile was distorted from a constant value, (i.e., the amount of boundary layer formed). Knowing this they were able to find an equivalent plate which would produce the same effect in the analog problem. Thus they were able to calculate the surface age.

Though they gave a treatment for the surface age, (and showed that errors up to 20 per cent could arise) they did not use it in presenting their data in graphical or tabular form. This raises the question as to the validity of the main conclusion that they reached: the rate of attainment of equilibrium was dependent upon the orifice and jet velocity.

The author has some reservation to this. It is felt that possibly different conclusions might have been reached if the effect of non-uniform velocity profile had been taken into account and in particular there is some doubt as to the design of their orifice. In the preliminary stages of this study attempts were made to produce orifices in the same manner as Rideal and Sutherland. They heated capillary tubing, then squeezed it to produce an elliptical section. Then the capillary tubing was sealed to tubing of 5 mm. internal diameter, and the capillary was cut off as close to the joint as possible. None of these orifices gave consistent results for pure liquids. A satisfactory seal was never obtained such that the entrance to the orifice was perfectly symmetrical. It is the

author's experience that orifices made in this manner are unsatisfactory. When ink was introduced into the fluid flowing into the orifice, it was observed that the stream lines formed gave a complex flow pattern for two or three diameters from the entrance of the orifice. As the orifice is made shorter it became apparent that this turbulent region may extend into the jet proper and the requirement for laminar flow was not met. In particular their orifice A which has a ratio of length to diameter $\frac{l}{d}$ of 3 gave results which depended on the flow rate. It should be noted that the difference in their results decreased as the distances from the orifice was increased, which would be expected if there was initial turbulence which was damped by viscous forces as the distance from the orifice increased. If the turbulent region in the orifice extends into the jet then the comparison of data obtained from their orifice K ($\frac{l}{d} = 6$) and orifice A would be invalid on the grounds that the jet from the orifice K would be laminar flow.

B. Extension of the Method for Surface Tension Measurement to Jets of Non-Uniform Velocity Profile

The most recent treatment of theory of vibrating jets was given by Hansen, Purchase, Wallace, and Woody (25). They presented a solution to the problem of estimation of surface age from measured axial distance and of surface tension from

measured wave lengths in jets of varying axial velocity profiles.

The surface age problem is treated in terms of an unperturbed cylinder. They let r, Θ, z be the cylindrical coordinates of an element in the jet, taking z = 0 at the orifice. They used the following notation: let r_o (cm.) be the stream radius, Q ($cm.^3/sec.$) the volume discharge rate, v_o (cm./sec.) the mean axial velocity, t (sec.) the time elapsed since a given element left the orifice, v (cm./sec.) the axial velocity of that element, and ρ ($gm./cm.^3$) and μ (poises) the liquid density and viscosity respectively. Then they defined the following dimensionless groups for more convenient notation: $V = \frac{v}{v_o}$, $\tau = \frac{\mu t}{\rho r_o^2}$, $y = \frac{r}{r_o}$, and $Z = \frac{\mu z}{\rho v_o r_o^2}$

They combined an equation due to Bohr (6), which gave the velocity profile of the cylindrical jet stream as a function of y and τ, i.e., $V(y,\tau)$, with an approximate treatment due to Schiller (43) which gave the development of the velocity profile within a cylindrical pipe (i.e., the orifice). Thus knowing the length of the orifice x, the radius of the orifice r_o and the Reynolds number R, the velocity profile at the pipe's orifice (i.e., V (y, 0) could be predicted) and the velocity profile in the jet stream as function of y and τ was fixed. The quantity $y' = \frac{r'}{r_o}$ represented the fraction of the radius of the stream inside the orifice that had a constant velocity profile and was expressed as a function of the single

dimensionless group $\frac{x}{r_o R}$. Over the range of greatest practical interest ($y' < .75$), y' was given analytically in terms of $\frac{x}{r_o R}$ to excellent approximation by $y' = 1-2.26 \left(\frac{x}{r_o R}\right)^{0.375}$. Rather complex equations were developed for $V(1,\tau)$ and $Z(1,\tau) = \int_0^{\tau} V(1,\tau')\, d\tau'$ which related surface velocity and axial distance to surface age. These equations were evaluated for various values of y' by using an IBM 604 computer, and the function $V(1, Z)$ (surface velocity as a function of axial distance) was established by graphical comparison of the function $V(1,\tau)$ and $Z(1,\tau)$. The functions $V(1,\tau)$ and $Z(1,\tau)$ are given in Tables 1 and 2 for the range $.1 \leq y' \leq .8$. The function $V(1, Z)$ and $\tau(1, Z)$ are presented graphically in Figures 1 and 2 for various values of the parameter y'.

The problem of determining an exact or even reasonably approximate solution of the problem in mathematical hydrodynamics presented by the vibrating jet with non-constant velocity profile appeared impractical and hence the problem was considered from the standpoint of the principle of similitude. The velocity profile of the jet must depend on orifice length, x, the axial distance z from the orifice, the surface tension, γ, wave length, λ, mean radius, r_o, mean velocity, v_o, viscosity, μ, the density of the liquid, ρ, and the amplitude b. Hence a functional relation must exist between γ, r_o, λ, v_o, b, μ, ρ, x and z, (9 variables) but since there are three independent dimensions in the problem (mass, length and time) this functional relation must reduce to one involving only 6

Table 1

Tabulation of V $(1,\tau)$ as a function of the parameter y' in the range $.1 \leq y' \leq .8$

V

τ /y'	.1	.2	.3	.4	.5	.6	.7	.8
.020	.525	.550	.580	.610	.652	.696	.750	.875
.040	.684	.699	.726	.742	.774	.811	.854	.946
.060	.774	.786	.802	.821	.844	.872	.912	.966
.080	.836	.845	.857	.871	.889	.919	.931	.979
.100	.879	.886	.895	.904	.919	.934	.950	.985
.120	.910	.916	.922	.930	.942	.951	.963	.990
.140	.933	.935	.942	.948	.956	.964	.973	.991
.160	.950	.953	.957	.961	.967	.973	.980	.994
.180	.963	.965	.968	.971	.976	.980	.985	.996
.200	.972	.973	.976	.979	.982	.985	.989	.997
.220	.979	.981	.982	.984	.987	.989	.992	.998
.240	.985	.986	.987	.988	.990	.991	.994	.998
.260	.989	.989	.990	.991	.993	.994	.996	.999

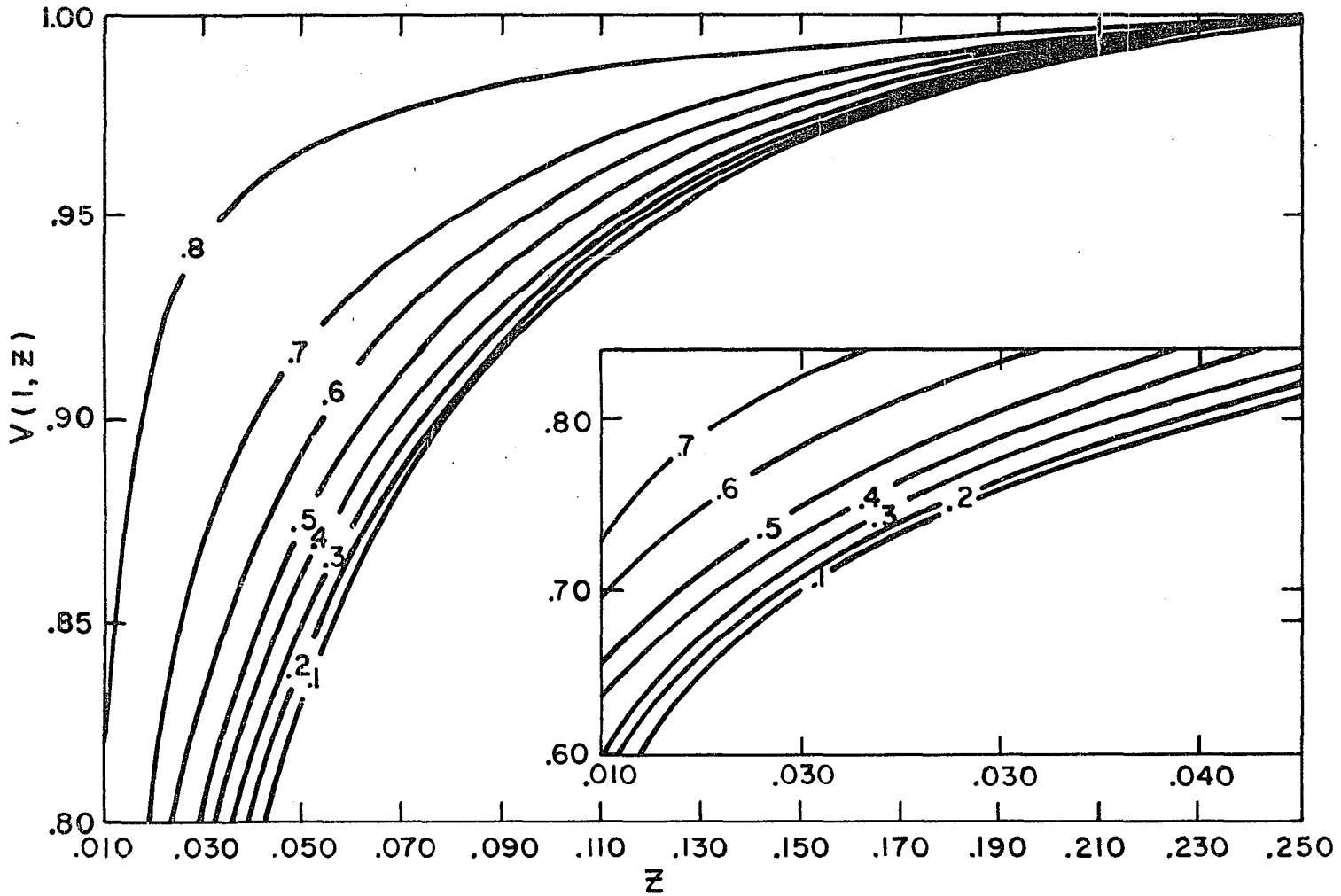

Figure 1. Plot of V (1, Z) versus Z for the range of values $.1 \leq y' \leq .8$

Table 2

Tabulation of Z $(1,\tau)$ for values of τ as a function of the parameter y' in the range $.1 \leq y' \leq .8$

Z

τ /y'	.1	.2	.3	.4	.5	.6	.7	.8
.020	.0075	.0077	.0081	.0087	.0096	.0105	.0116	.0150
.040	.0199	.0204	.0212	.0222	.0236	.0255	.0279	.0334
.060	.0345	.0354	.0365	.0380	.0399	.0424	.0455	.0526
.080	.0507	.0517	.0531	.0549	.0572	.0604	.0638	.0752
.100	.0678	.0690	.0706	.0727	.0753	.0786	.0826	.0917
.120	.0857	.0871	.0888	.0991	.0939	.0975	.1018	.1114
.140	.1042	.1056	.1075	.1098	.1128	.1166	.1211	.1312
.160	.1222	.1245	.1265	.1290	.1321	.1360	.1406	.1511
.180	.1413	.1437	.1457	.1483	.1515	.1555	.1603	.1710
.200	.1607	.1631	.1651	.1678	.1711	.1752	.1800	.1909
.220	.1802	.1826	.1847	.1874	.1908	.1949	.1998	.2108
.240	.2000	.2023	.2044	.2072	.2112	.2147	.2197	.2308
.260	.2171	.2220	.2242	.2269	.2304	.2343	.2396	.2500

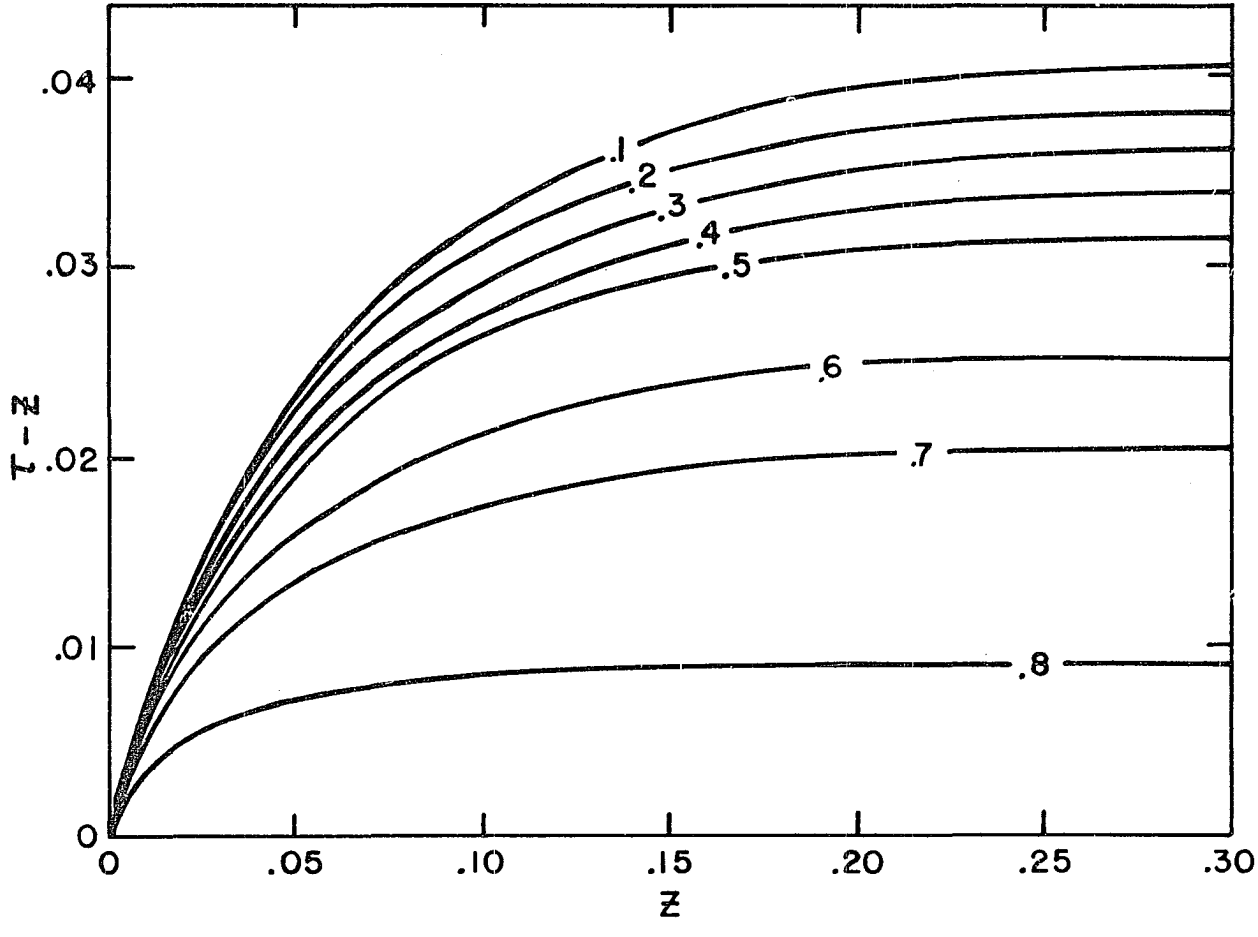

Figure 2. Plot of τ - Z versus Z for the range of values $.1 \leq y' \leq .8$

independent dimensionless groups, choice of which is arbitrary so long as all are independent (31). One is at freedom to pick 4 of these groups such that they satisfy Bohr's (6) equation for axial velocity constant across the jet section, i.e.,

$$\psi = \frac{1}{6}\phi_1^2\left\{1 - \frac{5}{12}\phi_1^2 + \frac{85}{576}\phi_1^4 + 2\phi_2^{3/2} + 3\phi_2^2 + \frac{37}{24}\phi_3^2\right\}$$

in which $\psi = \frac{\gamma}{\rho v_o^2 r_o}$, $\phi_1 = \frac{2\pi r_o}{\lambda}$, $\phi_2 = \frac{2\mu}{\rho v_o k r_o^2}$, $\phi_3 = \frac{b}{r_o}$ (1)

This equation assumes terms in ϕ_1^4, $\phi_2^{3/2}$, ϕ_2^2, and ϕ_3^2 second order compared to ϕ_1^2 and that contribution due to the density of the air is negligible and is then accurate to second order. The remaining two groups suggested by the variables listed are

$$\phi_4 = \frac{x\mu}{\rho v_o r_o^2}, \quad Z = \frac{z\mu}{\rho v_o r_o^2}$$

Although the tabulation of a function of five variables is a formidable task, it is possible (although of course not required by the principle of similitude) that the function be separable, and in particular that it may depend on ϕ_1, ϕ_2, and ϕ_3 as indicated by Bohr's equation, and on the remaining two dimensionless groups through a correction factor involving only these groups. It may also be possible to choose such a dimensionless group that the correction factor depends on it alone, i.e., on a single variable. The possibilities are summarized in the

equation,

$$\Psi = \Psi_o (\phi_1, \phi_2, \phi_3) f (\phi_5) \qquad (2)$$

where the function $\Psi_o (\phi_1, \phi_2, \phi_3)$ is given by equation 1. ϕ_5 remains to be specified and $f (\phi_5)$ to be determined.

The fact that surface velocity differs considerably from the bulk velocity near the orifice and the fact that the determination of the ratio $\frac{v_s}{v_o} = V (1, Z)$ is dependent on the functions ϕ_4 and Z leads one to select $\phi_5 = V (1, Z)$ and $f (\phi_5) = V (1, Z)^n$ where the n is to be determined experimentally using a number of different orifices, liquid and flow rates.

In the study of Hansen, Purchase, Wallace and Woody (25) results were obtained with orifice length to diameter ratios, surface tension, densities, viscosities, and flow Reynold numbers varying by factors of approximately 3, 3, 3, 25, and 2 respectively. It was found that n was equal to .63 $\pm$ .01. The excellent correlation they found for their data constituted a justification of the assumptions used in the dimensionless treatment.

In summary, they recommend the following equation for the calculation of surface tensions of pure liquids from measurements of vibrating jets:

$$\gamma = \frac{2}{3}\rho\frac{\pi^2 v^2 r^3}{\lambda^2}\left\{1 - \frac{5}{3}\left(\frac{\pi r}{\lambda}\right)^2 + \frac{85}{36}\left(\frac{\pi r}{\lambda}\right)^4 + 2\left(\frac{\mu\lambda}{\rho v \pi r^2}\right)^{3/2}\right.$$

$$\left. + 3\left(\frac{\mu\lambda}{\rho v \pi r^2}\right)^2 + \frac{37}{24}\left(\frac{h}{r}\right)^2\right\} \quad V(1, Z)^{.63} \qquad (3)$$

in which V (1, Z) is obtained from Figure 1 for the corresponding value of y', determined by $\frac{x}{Rr_o}$.

It has yet to be shown that this equation will equally well represent the surface tension time dependence of surface active aqueous solutions and that the results obtained will be independent of the orifice used. Once the dependence of the surface tension on the distance from the orifice has been established, Figure 2 may be used to find the dependence of surface tension on time.

C. Kinetics of Adsorption

Bond and Puls (8) were apparently the first to give a semiquantitative theory of adsorptive process based on a diffusion controlled mechanism. They defined a characteristic time which was the time required for the surface tension to pass halfway to its equilibrium value. The depth of solution that would have to be denuded would be of the order Γ/c where Γ is the surface excess in moles/cm.^{2}, and c is the bulk concentration in moles/cm.^{3}, then with the use of Gibbs' equation they obtained that $\Theta = (\Gamma/c)^2/D = \frac{(-d\sigma/dc)^2 c \to o}{DR^2T^2}$

where D is the diffusion coefficient.

Then coupling Gibbs' equation with Szyszkowski's equation and assuming that in dilute solution $\gamma_o - \bar{\gamma}$ (i.e., surface tension of water minus the surface tension of the aqueous solution at equilibrium) was proportional to c, which was in turn assumed proportional to Γ, arrived at the equation:

$$\frac{(\gamma_o - \bar{\gamma}) - (\gamma_o - \gamma(t))}{\gamma_o - \bar{\gamma}} = \exp\left(-\frac{2}{\sqrt{\pi}}\sqrt{\frac{t}{\theta}}\right) \qquad (4)$$

where $\gamma(t)$ is the surface tension at time t. A test of this equation is to plot $\log \frac{\gamma(t) - \bar{\gamma}}{\gamma_o - \bar{\gamma}}$ vs. $\sqrt{t}$. It should be noted that their limiting assumption that the adsorption layer could be supposed to be almost unoccupied and $\Delta\gamma$ proportional to c restricts their treatment to the initial stages only of the diffusion process and low concentrations. They conclude that their data for soap solutions determined by the vibrating jet method and Harkins and Brown's (27) data for decylic acid solutions agreed with equation 4. It is maintained here that the results are largely fortuitous; for if a plot of $\log \frac{\gamma(t) - \bar{\gamma}}{\gamma_o - \bar{\gamma}}$ vs. $\sqrt{t}$ is made and compared with a plot corrected[1] for surface age it is apparent that a linear relation in t will also suffice

---

[1] In order to make this correction it was necessary to make a few justified assumptions since they gave insufficient data in their paper. The radius (.082 cm.) and the time in seconds for a given depression were given by them. From an earlier paper by Bond (7) it was possible to estimate that the effective length of the orifice was approximately .40 cm. From the fact that they used a horizontal jet, they would have needed the highest velocity (in order to have less curvature in the stream) (cont'd. on next page)

to explain the data. Successful application of their equation to the data of Harkins and Brown is again fortuitous because these data provided almost no information concerning the critical initial dependence of surface tension on time. Neither the data of Bond and Puls or of Harkins and Brown, therefore, provide definitive evidence for a diffusion controlled rate process.

Boutaric and Berthier (9) found that their data for the surface tension time dependence of saponin solutions could also be fit by an equation of the form

$$\frac{\gamma - \gamma_\infty}{\gamma_o - \gamma_\infty} = \exp(-at) \qquad (5)$$

Ward and Tordai have written a series of papers on the problem of kinetics of adsorption at interfaces. In 1944 they (51) concluded from their study on the rate of fall of the interfacial tension between water and solutions in hexane of long chain amphipathic substances that the diffusion to the interface only accounted for a very small fraction (about 10^{-8})

(cont'd. from previous page) possible consistent with the condition

$$R = \frac{\rho v_o r_o}{\mu} \leq 2{,}000.$$

Thus one may assume v_o is approximately 200 cm./sec. With this it is apparent that $y' = .75$ and one is able to draw a z(cm.) vs. t(sec.) curve with the aid of Table 2. Then using the times of their data and multiplying them by the velocity, one obtains the corresponding z(cm.) which is used to find the corrected time from the z(cm.) vs. t(sec.) curve.

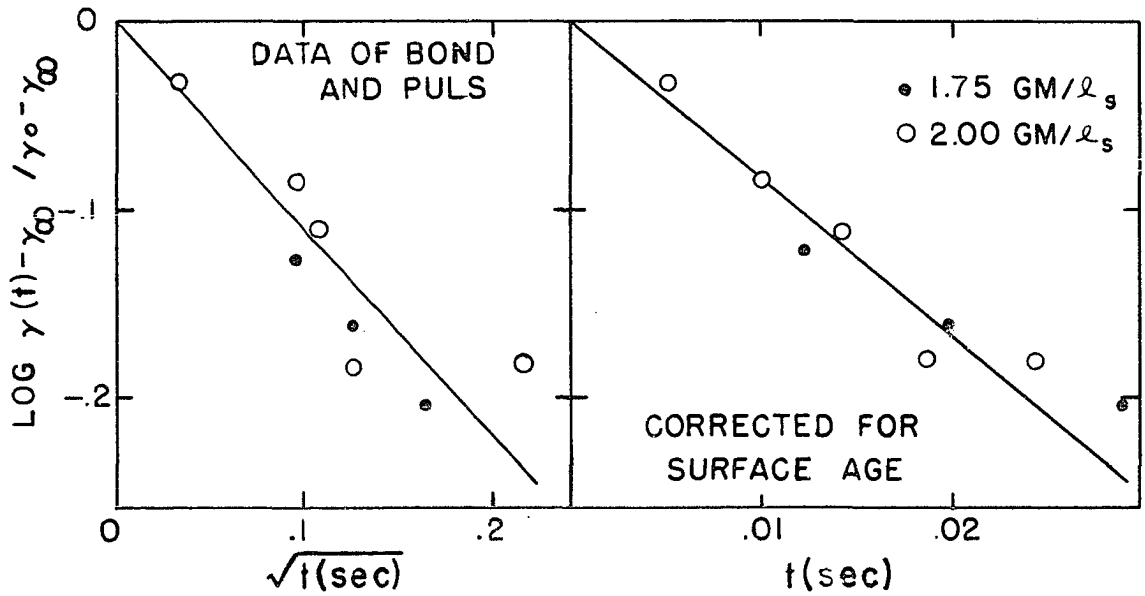

Figure 3. Comparison of rate law on the dependence on $\sqrt{t}$ for uncorrected surface velocity with dependence on t for corrected surface velocity

of the time required. They calculated that with lauric acid as the solute, a diffusion coefficient as low as 10^{-22} cm.^{2}/sec. would be required instead of the actual value of 10^{-5} cm.^{2}/sec. if diffusion was the rate controlling step. They proposed that the diffusion to the surface is followed by a process of high activation energy to produce the final state of the surface film and concluded that the activation barrier also affects desorption as well as adsorption of molecules.

Later they (52) proposed a quantitative theory on the effect of diffusion on the variation of the surface tension with time. The general theory of diffusion to the surface that they derived allowed for back diffusion and no assumptions of a physical nature were necessary. Their theory gave the surface concentration M (moles/cm.^{2}) at the time t as

$$M = 2\left(\frac{D}{\pi}\right)^{\frac{1}{2}} \left\{ n_o t^{\frac{1}{2}} - \int_0^{t^{\frac{1}{2}}} \phi(z)\, d\left[(t - z)^{\frac{1}{2}} \right] \right\} \qquad (6)$$

where D (cm.^{2}/sec.) was the diffusion coefficient, n_o was the bulk concentration in moles/cm.^{3} and $\phi(z)$ was the concentration in subsurface which varied with the time in some unknown manner. They were able to obtain M or D if one or the other was known, but the equation could not be integrated explicitly as $\phi(z)$ was not known explicitly. They devised a scheme where by using surface tension depression rate data they calculated a diffusion coefficient D_c. Then by comparing D_c with the experimental D_e some conclusions could be drawn as

to the controlling step. They concluded that the rate of adsorption in the series pentanoic through octanoic acids was not diffusion controlled, but controlled by some barrier at the surface.

Burcik (12, 13, 14, 15) and coworkers have applied the vibrating jet method to measure the rate of lowering of surface tension of detergent solutions. They derived no rate laws and only indicated relative trends. It should be pointed out that they did not correct for surface age or non-uniform velocity profiles. More recently Ross and Haak (42) have used the vibrating jet in a study on the inhibition of foaming. Again the surface age was incorrectly calculated, but since they were giving a qualitative, relative treatment this error was less important.

Posner and Alexander (35, 36) have applied a surface potential technique, based on the vibrating jet method, to the study of the kinetics of adsorption of a series of n-aliphatic alcohols (butyl, heptyl, octyl) at the air-water interface. They found that under almost all conditions the experimental results fitted the equation

$$\ln (V_E - V) = -kt + \text{constant} \qquad (7)$$

where V_E = equilibrium surface potential, V = surface potential at time t, and k a constant (of dimensions sec.^{-1}) at each concentration. They followed the lead taken by Rideal

and Sutherland (41) and assumed that the adsorption of solute would be due to flow processes in the jet coupled with an energy barrier to entry into the surface. Since the effect of the flow process should be of lesser importance near the jet orifice they considered the data obtained there independently of the rest. For example, they observed that by extrapolating the curves of ln (V_E - V) - t to zero time, the intercept was found to be less than the value of V_E predicted by equation 7. They maintained that the difference was caused by lack of stirring near the orifice. It should be noted that this stirring would have been complete in less than .001 seconds.

They considered two models to account for their data after the initial stages. (1) Diffusion through a stirred layer without energy barrier to surface and (2) hindered film penetration. They rejected the first proposal on the basis that a faster equilibrium was predicted by the diffusion case than was observed. Consequently they interpreted their fundamental rate law on the basis of a Langmuir type hindered adsorption.

They let Θ be the fraction of surface covered at time t, k_1 be the velocity coefficient of adsorption (dimensions $cm.^3$/molecule-sec.), c be the concentration in the bulk solution (molecule/$cm.^3$) and k_2 be the velocity coefficient of desorption ($cm.^3$/molecule-sec.) thus the rate equation was written as

$$\frac{d\Theta}{dt} = k_1 C (1 - \Theta) \frac{-k_2 n_f}{\delta} \Theta \qquad (8)$$

where n_f = the number of molecules/cm.^{2} when the molecules were close packed on the surface and δ was the thickness of the surface layer in cm. By noting that at equilibrium $\frac{d\Theta}{dt} = 0$, and $\Theta = n/n_f$, the equation may be revised to

$$\frac{dn}{dt} = n_E (k_1 c + k_2 \frac{n_E}{\delta}) - (k_1 c + k_2 \frac{n_E}{\delta})_n$$

$$= (k_1 c + k_2 \frac{n_E}{\delta}) (n_E - n) \qquad (9)$$

which upon integration yielded

$$\ln (n_E - n) = -(k_1 c + k_2 \frac{n_E}{\delta})t + \text{constant} \qquad (10)$$

which then reduced to

$$\ln (\Delta V_E - \Delta V) = -(k_1 c + k_2 \frac{n_E}{\delta})t + \ln \Delta V_E \qquad (11)$$

They observed that with increasing chain length, k_1 increased and k_2 decreased. They made a temperature study on k_1 and k_2 and found both increased with temperature but k_2 much more so than k_1. From the temperature variations the activation energies for the forward and reverse process (E_1 and E_2 respectively) were calculated from the Arrhenius equation.

From the Langmuir theory of hindered adsorption, E_1 would presumably represent the energy to make a "hole" of appropriate size to enable the penetrating molecule to enter the surface film. In view of the coiling up which hydrocarbons chains undergo when dissolved in water, an approximate constancy of E_1 was expected. Since E_2 would be the sum of E_1 and ΔH, where ΔH is the energy liberated when the hydrocarbon chain goes from the aqueous to the surface phase, E_2 should increase with chain length.

Rideal and Sutherland (41) have given numerous examples of diffusion mechanism with and without stirring, with and without energy barriers, and have applied these to their data found by the vibrating jet method. As pointed out earlier they do not believe the vibrating jet method can be used to study kinetics of adsorption, but it appeared to them that the process should be diffusion controlled coupled with an energy barrier to entry for the longer chained compounds. In contrast to the solution of the basic diffusion equation obtained by Ward and Tordai (52), they needed to make the physical assumption that the surface concentration was directly proportional to the subsurface concentration. This is equivalent to assuming the surface layer obeys ideal conditions (no such case exists) and is applicable only at small concentrations.

Purchase (38) has recently made a study on the kinetics of adsorption of various detergent systems and arrives at the conclusion that the process was diffusion controlled. It is felt

that the physical assumptions made by her to solve the basic diffusion equation were more realistic than those of Rideal and Sutherland. In order to fit her experimental data, she needed to define a diffusion coefficient, an order of magnitude lower than expected (i.e., 10^{-7} cm.^{2}/sec. where one would expect 10^{-6}). She had correctly calculated the surface age. The majority of her data occurred in the range where most of the surface tension depression had occurred. Thus she could not resolve whether her mechanism held for low concentrations. If a diffusion coefficient of the expected order of magnitude is used, her data would compliment that given in this work and the same conclusions would be reached as given in this work.

Sutherland (49) has studied the rates of adsorption of decanol and lauric acid and concluded that the controlling step was passage over an energy barrier into the surface from a stirred solution. He finds an activation energy of 16RT for lauric acid and approximately 15RT for decanol.

From this survey it is concluded that there is no strong evidence for the diffusion controlled mechanism. It appears to the author that all of the evidence points to the passage over an energy barrier as the controlling mechanism with the diffusion process being of little importance.

III. MATERIALS

The four fatty acids, n-heptanol and the sec-butyl alcohol used in this research were best grades Eastman chemicals. The methanol which was Baker and Adam's Reagent grade absolute methanol, the ethanol which was Commercial Solvent's Gold Schield TS grade, and the 2-butanol were further purified in the manner of Lund and Bjerrum (30_a). The distilled water was redistilled from alkaline permanganate solution. All organic compounds were further purified by distillation through a 30-plate Oldershaw column at reflux ratios in excess of 10-1. The boiling ranges of the central fractions used in this work, corrected to 760 mm. were

Compound	Boiling range
2-Butanol	99.4- 99.7
Ethanol	78.3- 78.5
Heptanoic acid	222.9-223.5
n-Heptanol	175.6-176.1
Hexanoic acid	203.6-204.5
Methanol	64.5- 64.6
Octanoic acid	236.6-237.4
Valeric acid	186.7-187.1

IV. EXPERIMENTAL INVESTIGATION

A. Measurement of Dynamic Surface Tension

1. Production of the jet

In order to produce stable vibrating jets from which accurate dynamic surface tension data may be obtained, the following requirements must be met:

a. The rate of discharge from the orifice must be constant.

b. The cross section of the internal bore of the orifice must be of the form $r = a + b \cos 2\Theta$ along its length and the entrance and exit faces of the orifice must be perpendicular to the axis of the orifice.

c. The orifice should be isolated from external vibrations.

The apparatus used to produce jets in this study was a modified form of that used by Purchase (38) and is shown in Figure 4.

The main reservoir A was a 5 liter, round bottom flask to which the discharge tube C was joined. A ground glass magnetic seat valve B was put in the discharge tube about 6 cm. from the reservoir to control the flow of liquid to the constant head reservoir D. The discharge tube was constricted at the bottom so that the rate of flow from the main reservoir just slightly exceeded the flow out the orifice tube G through the

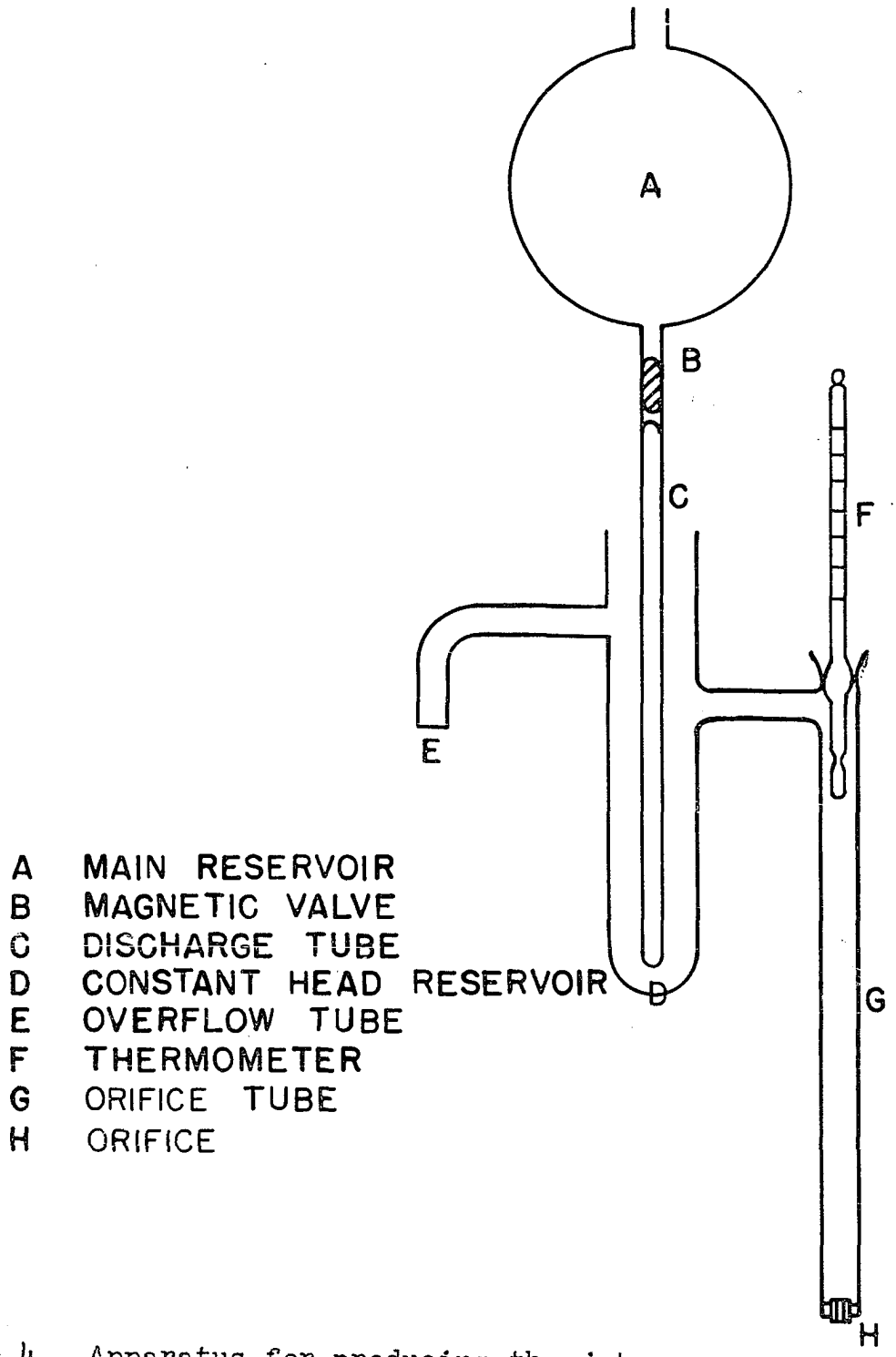

Figure 4. Apparatus for producing the jet

orifice H. The excess flow passed out the overflow tube E. A thermometer well was joined to the top of the orifice tube to hold the thermometer F. The entire system except for the cork retainer holding the orifice in the orifice tube was made of glass. A number of constant head reservoirs were made with varying lengths of orifice tubes so that a range of discharge rates through the orifice could be obtained.

In order to prevent turbulence in the constant head reservoir from affecting the jet, liquid was discharged into it near the bottom at an appreciable distance from the side tube through which the liquid flowed to the orifice tube. An investigation was made to see if the presence of the thermometer in the orifice tube causes any turbulence. Since the ratio of the dameter of the orifice to the diameter of the orifice tube was 1/15, the velocity of the liquid in the orifice tube is approximately 1/225 that in the orifice. Any turbulence set up would be localized and soon damp out as it moved down the tube. To check, ink was introduced into the side tube that leads to the orifice tube and the stream lines formed were observed. There were no irregularities or eddys anywhere along the thermometer.

Vibrations in the apparatus were reduced to a minimum by mounting the parts on a rigid frame. The framework, shown in Figure 5, was made from DexAngle, manufactured by Acme Steel Company.

The orifices used in this study were designed to meet the

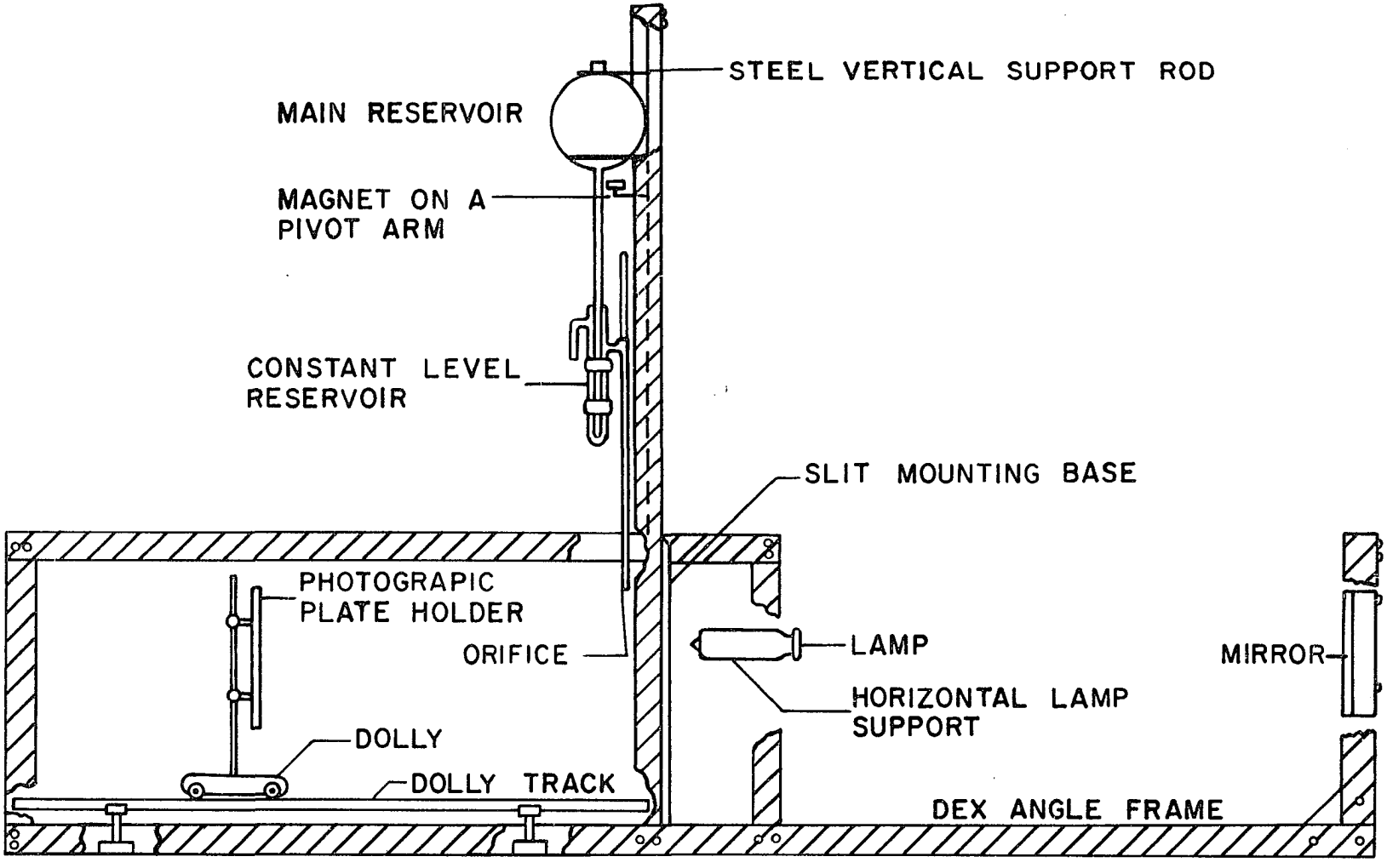

Figure 5. Schematic arrangement of apparatus on DexAngle framework

requirements of the theoretical treatment. The first requirement is that the orifice must be of known length and constant cross section. In addition, both faces of the orifice must be perpendicular to the axis of the orifice and the edges must be sharp 90 degree angles. The second requirement is that the cross section of the orifice should be of the form $r(\Theta) = a + b \cos 2\Theta$ where b/a is small. Purchase (38) developed a method for electroforming nickel orifices but the method does not produce orifices which meet the first requirement given above.

The glass orifices were formed by shrinking pyrex capillary tubing down onto a shaped steel mandrels. The mandrels were shaped from precision drill rod (.040" diameter) by the method described by Purchase.

The capillary tube that was to be shrunk was joined at both ends to 5 mm. tubing. The mandrel was then slipped into the capillary and one end of the 5 mm. tubing was connected to a helium source and the other end to a vacuum pump. The vacuum pump was started and the system was slowly flushed with helium. Then with the helium still flowing, the capillary tube was slowly heated up with a hand torch until all moisture had been expelled. The helium end of the system was then sealed off, the system evacuated, and then the pump side of the system was sealed off. The sealed system was then put into a horizontal tube furnace and slowly heated to 675°C. and left there for one hour. The system was then cooled. If careful temperature

control of the furnace was maintained, the mandrel could be removed from the capillary.

The shaped capillary tube was then checked for constancy of cross section by measuring the length of a mercury column as it was moved from one end of the tube to the other. The most constant section was then marked off on the capillary and the orifices were cut from this section by a conventional glass knife.

The newly cut orifices were first checked by microscope to inspect the cross section and to make sure that the cut faces were perpendicular to the axes of the orifice. The next test was to observe the length of the stable jet. Only those orifices with jets of a length in excess of 12 inches were kept. Next the orifice was tested in the apparatus to see if it gave the characteristic optical focusing that is described in a later section.

The orifices listed in Table 3 were made during the course of this study and all were found to give consistent results.

Table 3

Physical dimensions of orifices

Orifice	Length (cm.)	Major radius (cm.)	Minor radius (cm.)	Mean radius (cm.)
D	.890	.0501	.0445	.0472

Table 3. (continued)

Orifice	Length (cm.)	Major radius (cm.)	Minor radius (cm.)	Mean radius (cm.)
E	.648	.0508	.0474	.0491
F	.646	.0513	.0481	.0495

2. Measurement of the wave lengths and radii of the jets

To measure the wave lengths of the jet accurately it is necessary to use the jet proper as a focusing lens. When the jet is illuminated by a narrow beam of parallel light rays, the respective antinodes act as cylindrical lenses and produce astigmatic images of a point source (48). When a vertical screen is placed behind the stream at a distance of one focal length, horizontal parallel lines of light appear which are perpendicular to the stream. Each line of light corresponds to a node, thus the distance between successive lines of light corresponds to a wave length. Figure 6 is a schematic representation of the light being focused by the stream.

There are two effects which cause the focal lengths of the successive nodes to increase with distance from the orifice. Firstly, the viscosity of the liquid causes the oscillations to be damped so that relative curvature of each node is decreased and hence the focal length increased. Secondly, the vertical jet is accelerated by the effect of gravity and this causes an increase in the distance between

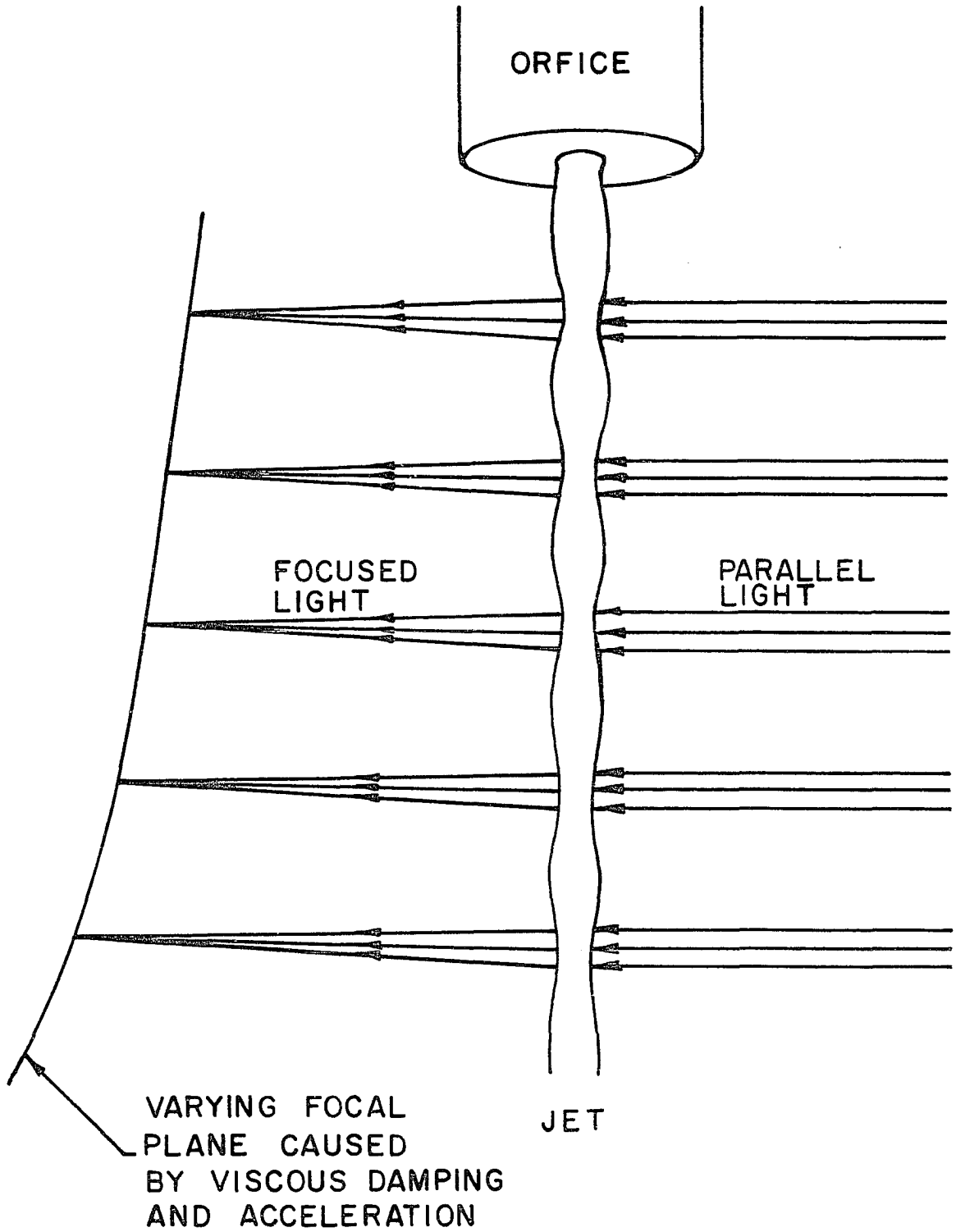

Figure 6. Focusing effect of the jet

nodes and consequently causes the focal length of the node to be further increased.

The parallel light was obtained by reflecting light of a point source from a parabolic mirror as shown in Figure 5. The mirror, which was ten inches in diameter with a focal length of seventy-six inches, was the one used by Purchase (38). The light source was a converted 40-watt "Zirconarc" photomicrographic lamp from the Fish-Schurmann Corporation. A point source was approximated by covering the bulb with aluminum foil and allowing the light to come through a 1/16" hole.

Since the focal length of the successive nodes increased with distance from the orifice, a photographic plate holder was attached to a dolly that moved on a track aligned parallel to the light beam so that successive photographs could be taken of the different regions of the focal surface formed by the jet. See Figure 5. Purchase (38, p. 62) has given an excellent photographic reproduction of an actual series of photographic plates taken during her studies; plates obtained in this work were of similar character.

The parallel light beam was further collimated by a vertical slit which was just wide enough to illuminate the vertical jet. See Figure 5.

In general, the distance of the focal surface from the jet increased as the surface tension of the solution decreased. It was always possible to get three successive lines in sharp enough detail to be measurable. By this means, a series of

photographs would overlap and all of the measurements could be consistently correlated.

Experiments were always performed in a completely darkened room and in addition, Masonite sheets were attached to the sides, top, and back end of the DexAngle frame to prevent reflected light from the walls and ceiling of the room from fogging the photographic plate when the exposures were made.

In order to determine the velocity of the jet it was necessary to know its diameter. This was done by photographing the jet stream and a cylindrical gauge in the same plane with a camera equipped with a 75 mm. f/2.3 Balter lens. This camera gave a magnification of 8X. Relative measurements were made from the photographic plate; then knowing the diameter of the gauge, the diameter of the stream was calculated.

All measurements to determine wave length or jet diameter were made by means of a Cambridge Universal Measuring Machine. This is essentially a traveling microscope with an accurate scale. The manufacturer states the machine is capable of measuring with a precision of 2×10^{-4} cm.

B. Experimental Procedure

Before each run, the glass assembly for producing the jet was disassembled and thoroughly cleaned with soap solution and water, rinsed with dilute hydrofluoric acid solution, rinsed again with distilled water and finally rinsed with acetone.

The orifice was given special treatment when the time depression runs were made with the surface active solution. It had been observed that with the lower discharge rates the jet would wet the face of the orifice thus forming a small frustrum with a base diameter about $1\frac{1}{2}$ times larger than that of the orifice extending about $1\frac{1}{2}$ mm. down the jet. It was observed that surface elements of this frustrum were essentially stagnant and hence the surface tension was essentially that of the equilibrium value. When the orifice was treated with Beckman "Desicote", a silicone based water repellent, the face was no longer wetted and the region of stagnation was eliminated. It has been shown by Brockman (10) that the hydrodynamical flow in a polyethelene tube was the same as in a brass tube. Thus one would expect the flow character in the clean glass orifice and the "desicoted" orifice to be identical, but the frustrum would be eliminated. This was observed to be true.

At the beginning of the test all the parts were assembled and the reservoir filled with the liquid to be tested. The jet was allowed to flow long enough so the stream could be adjusted to flow vertically. This was done by aligning the image of the jet and slit system on a screen in the plate holder and simultaneously aligning the stream with a plumb line in a 90^{o} direction from the light path. Next the jet was rotated until the horizontal bands of light were focused on the screen. It was found that the best focus could be obtained by observing the first line and bringing it into focus with the screen as

close to the jet as possible. Finally the plate holder was moved to various distances from the jet and those positions were marked to determine at which distances the photographs should be made in order to get overlapping results.

The timer on the light source was set and then the room was completely darkened. A photographic plate (4" X 10" M Spectrographic plate from Eastman) was then put into the plate holder and exposed for 1/10 of a second by the means of the timer. As the distance from the jet was increased, it was found that the exposure time had to be increased to 1/5 of a second.

After a series of plates were exposed, they were developed for 4 minutes in Eastman Kodak D-19 Developer, rinsed under running water and placed in Eastman Kodak F5A fixer for 8 minutes. After that they were washed in running water for 30 minutes and dried.

The distances of the lines from the orifice image were obtained by means of the measuring machine. Two measurements were made on each line and the two values averaged. For the sharpest lines the agreement was $\pm$ .03 cm. Fortunately, the calculation of the surface tension is not as sensitive to the distance of the lines from the orifice as to the actual distance between two successive lines.

The volume rate of flow was determined by measuring the length of time required to fill a 100 ml. volumetric flask. Two measurements were made in each test, one before and one

after the photographic plates were exposed. Agreement between measurements was $\pm$ .005 cm.^{3} per second.

For the first part of this study the tests were made between 24° and 28°C. The room temperature was 26° $\pm$ 2°C. The thermometer shown in Figure 3 was used to determine the average temperature of the jet. It was found that the temperature in the orifice tube agreed with that of the temperature of the fluid collected immediately beneath the orifice. For the time depression runs the liquid was cooled to below 20°C. and then allowed to warm in the main reservoir until the temperature of the fluid flowing through the orifice tube was 20.0 $\pm$ .3°C. For the lower temperature runs the deviation from the mean temperature was never greater than $\pm$ .6°C.

C. Procedure of Calculation

The observable quantities obtained were the weight of water discharged per second, w, the wave lengths, λ (cm.), the distance from orifice to the middle of the wave, z (cm.), the radius of the orifice at the vena contracta, a_o (cm.), the length of the orifice, x (cm.), the viscosity, μ (poises), and the density, ρ (gm./cm.^{3}).

The calculation of the apparent surface tension γ_a was fairly straight forward. First the discharge weight per second was converted to discharge rate Q (cm.^{3}/sec.) by dividing by

the density of the liquid. This was incorporated in the equation for the apparent surface tension to yield

$$\gamma_a = \frac{2}{3}\rho\frac{2}{\lambda^2 a}\left[1 - \frac{5}{3}\left(\frac{\pi a}{\lambda}\right)^2 + \frac{85}{36}\left(\frac{\pi a}{\lambda}\right)^4 + \frac{37}{24}\frac{b^2}{a^2} + 2\left(\frac{\mu\lambda}{\rho Q}\right)^{3/2} + 3\left(\frac{\mu\lambda}{\rho Q}\right)^2\right] \qquad (12)$$

For the water solutions the term $2\left(\frac{\mu\lambda}{\rho Q}\right)^{3/2} + 3\left(\frac{\mu\lambda}{\rho Q}\right)^2$ was practically constant and was set equal to .001. The term $\frac{37}{24}\frac{b^2}{a^2}$ was approximately equal to $\left(\frac{b}{a}\right)_{z=o}\exp\left(\frac{-4\mu z}{Q}\right)$. a_o corresponds to the radius at the vena contracta and a corresponds to the radius of the stream as a function of the distance from the orifice. For orifice D, a_o was equal to $.0460 \pm .0002$.

The problem of determining a as a function of the distance z from the orifice was difficult. From consideration of first principles (i.e., conservation of mass, $\pi\rho v_o a_o^2 = \pi\rho v a^2$ and conservation of energy $\rho v^2 = \rho v_o^2 + 2\rho gz$) it would appear that a should vary according to the equation $a = a_o\left(1 + \frac{2gz}{v_o^2}\right)^{-\frac{1}{4}}$. This equation was tested by photographically determining the successive maxima and minima diameters of the jet as a function of distance from the orifice. The average diameter at a point z was found by taking the average of the diameters on either side of the point z and then averaging this value with the diameter at point z. By experiments over a large range of viscosity and discharge rates it was found that $a = a_o$

$(1 + \frac{2gz}{v_o^2})^{\frac{1}{2}}$. This relation was used throughout. No reason for this deviation from the theoretical value could be found at this time.

The correction for the non-uniform velocity profile, V (1, Z) was found with the help of the following equations. First y' was found from the relation $y' = 1-2.26\ (\frac{x}{Rr_o})^{.375}$ where r_o is the mean radius of the orifice. Then a plot of V (1, Z) vs. Z was made by interpolation from Figure 1. The corresponding Z for each wave length was found from the relation $Z = \frac{\mu\pi}{\rho Q}.z$ where z is the distance from the orifice. Then the values of V (1, Z) were read from the graph, raised to the .645 power and multiplied by the apparent surface tension γ_a.

The values of the corresponding surface ages were obtained with the aid of Figure 2 and the value of y'. A table of τ vs. Z was obtained from Figure 2 for the corresponding value of y'. This was transformed to a graph of t(sec.) and z(cm.) by the relations $Z = \frac{z\rho Q}{\mu\pi}$ and $t = \frac{\rho r_o^2 \tau}{\mu}$ (horizontal jet). (See Figure 7). The horizontal curve was corrected for the acceleration of gravity to obtain a vertical jet time curve. This was done with the recurrence equation

$$Z_{vi} = Z_H - \frac{gt^2}{2}\, i - 1 \quad i = 0, 1, 2, \ldots . \qquad (13)$$

The process was repeated until a constant value of Z_{vi} was obtained for the largest distance. Figure 7 is an illustration

of a correction curve for horizontal and vertical jets.

The error in the experiment was computed by only considering the measurable factors of the controlling term (i.e., $\frac{2}{3}\frac{Q^2}{\lambda^2 a}$, this accounts for 95 per cent of the value of the surface tension). The maximum differential error was

$$\left(\frac{d\gamma}{\gamma}\right) = 2\left(\frac{dQ}{Q}\right) + 2\left(\frac{d\lambda}{\lambda}\right) + \left(\frac{da}{a}\right).$$

It was assumed that the density was known exactly. Hence for a discharge rate of 1.70 $cm.^3/sec.$

$$\left(\frac{d\gamma}{\gamma}\right) = .006 + .006 + .004 = .012$$

or an accuracy of 1.2 per cent.

Figure 7. Dependence of age of the jet on distance from the orifice

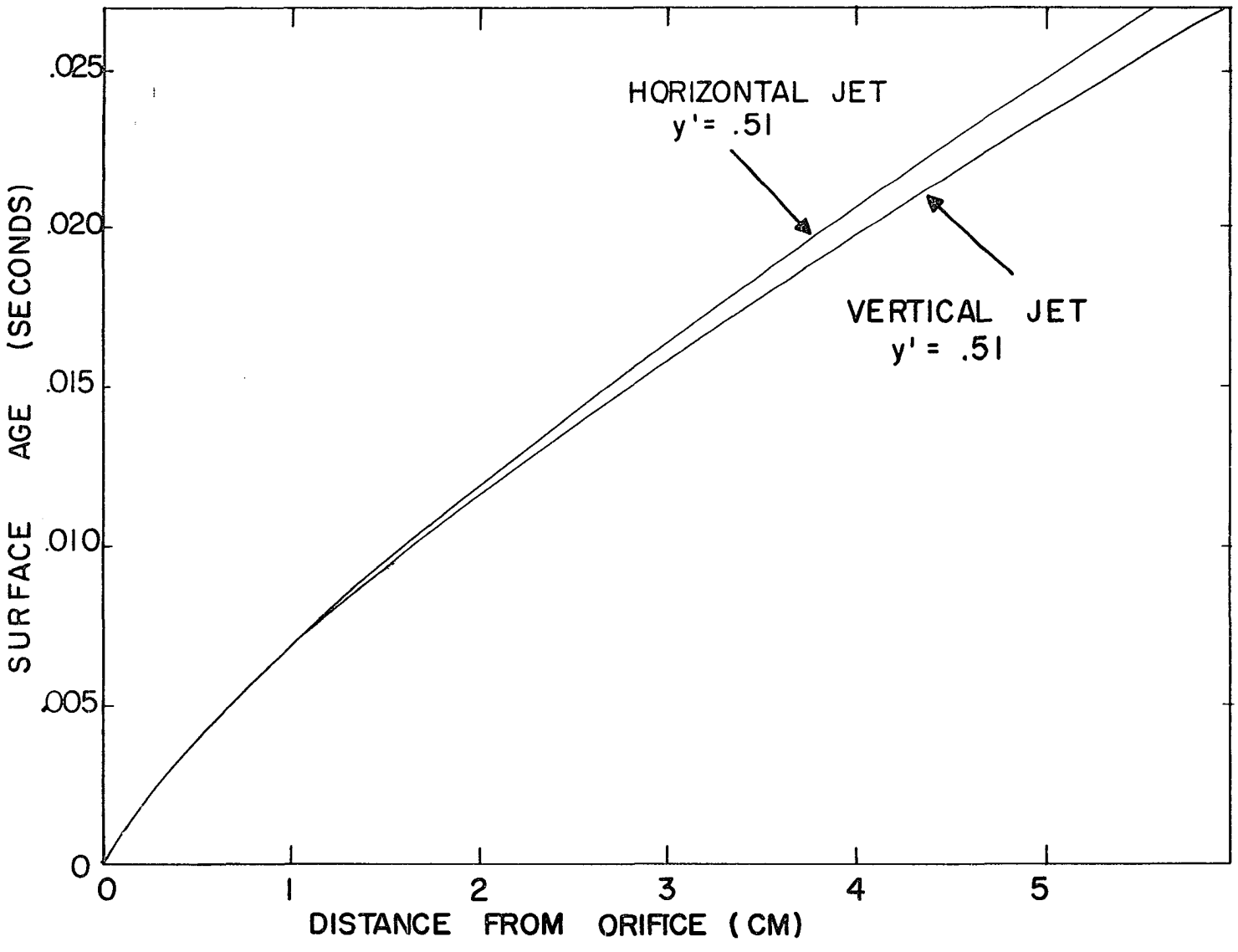
HORIZONTAL JET
y' = .51
VERTICAL JET
y' = .51
SURFACE AGE (SECONDS)
.025
.020
.015
.010
.005
0
0
1
2
3
4
5
DISTANCE FROM ORIFICE (CM)

V. RESULTS

A. Determination of the Constant n

To check the theory of Hansen, Purchase, Wallace, and Woody (25) and determine the parameter n in equation 3 it was necessary to make a number of tests with different liquids and different orifices. This was broken into two sections. First using orifice D, which was used for the majority of the measurements, a number of tests were made with organic liquids having a large range of difference in their physical properties such as viscosity, density, and surface tension. Then using these data, the uncorrected equation was used to calculate an apparent surface tension, namely:

$$\gamma_a = \frac{2}{3} \cdot \frac{\rho Q^2}{\lambda^2 a} \left[1 - \frac{5}{3} \left(\frac{\pi a}{\lambda}\right)^2 + \frac{85}{36} \left(\frac{\pi a}{\lambda}\right)^4 + \frac{37}{24} \frac{b^2}{a^2} + 2 \left(\frac{\mu \lambda}{\rho Q}\right)^{3/2} + 3 \left(\frac{\mu \lambda}{\rho Q}\right)^2 \right] \qquad (14)$$

then dividing the static surface tension by this and taking the logarithm, it is clear that one has

$$\log \frac{\gamma_t}{\gamma_a} = n \log V = n \log \left(\frac{V_s}{V_o}\right) \qquad (15)$$

Thus a plot with log V as the abscissa and log $\frac{\gamma_t}{\gamma_a}$ as the ordinate should yield a straight line passing through the

origin with slope n. The data for $\frac{\gamma_t}{\gamma_a}$ and V are given in Table 4 and Figure 8a for the four organic liquids, benzene, 2-butanol, ethanol, and methanol.

Secondly, using orifices D, E, F, which had been "desicoted", a number of tests were made with water and then the same correlation procedure was used as in the first part. The data for $\frac{\gamma_t}{\gamma_a}$ and V (1, Z) are given in Table 5 and Figure 8b for the three orifices.

B. Dependence of the Dynamic Surface Tension of Water on the Temperature and Time

The dependence of the dynamic surface tension of water on the temperature and time was determined with orifice D which had been "desicoted". The results are given in Table 6 and Figure 9.

C. Independence of the Dynamic Surface Tension on the Orifice

The dependence of the surface tension on time was measured for four solutions of heptanoic acid in the concentration range from .00150 M/ls to .00750 M/ls for different orifices. The results are presented in Table 7, Table 8, and Figure 10.

Table 4

Dynamic surface tensions: benzene, 2-butanol, ethanol and methanol

Benzene

	Q=1.284 cm.^{3}/sec., T=28°C.				Q=1.412 cm.^{3}/sec., T=26°C.			
n	λ (cm.)	z (cm.)	$\frac{\gamma_t}{\gamma_A}$	$\frac{V_s}{V_o}$	λ (cm.)	z (cm.)	$\frac{\gamma_t}{\gamma_A}$	$\frac{V_s}{V_o}$
1	.778	.697	.855	.708	.830	.762	.800	.695
2	.800	1.500	.877	.807	.876	1.615	.864	.780
3	.826	2.319	.908	.844	.906	2.503	.897	.848
4	.843	3.152	.927	.882	.918	3.412	.914	.885
5	.858	4.003	.940	.909	.937	4.337	.929	.913
6	.867	4.863	.952	.929	.947	5.275	.938	.932
7	.900	5.725	.966	.945	.955	6.124	.948	.944

2-Butanol

	Q=1.492 cm.^{3}/sec., T=26°C.				Q=1.248 cm.^{3}/sec., T=26°C.			
n	λ (cm.)	z (cm.)	$\frac{\gamma_t}{\gamma_A}$	$\frac{V_s}{V_o}$	λ (cm.)	z (cm.)	$\frac{\gamma_t}{\gamma_A}$	$\frac{V_s}{V_o}$
1	1.064	.874	.959	.919	.893	.757	.948	.900
2	1.072	1.942	.989	.978	.898	1.653	.966	.956
3	1.082	3.019	.993	.995	.915	2.559	1.000	.995
4	1.090	4.101	.993	1.000	.924	3.479	1.000	1.000
5	-	-	-	-	.932	4.407	1.000	1.000

Table 4. (continued)

	Ethanol				Methanol			
	Q=1.590 cm.^{3}/sec., T=26°C.				Q=1.108 cm.^{3}/sec., T=25°C.			
n	λ (cm.)	z (cm.)	$\frac{\gamma_t}{\gamma_A}$	$\frac{V_s}{V_o}$	λ (cm.)	z (cm.)	$\frac{\gamma_t}{\gamma_A}$	$\frac{V_s}{V_o}$
1	1.050	.927	.848	.768	.690	.591	.796	.681
2	1.100	2.004	.907	.872	.721	1.300	.852	.786
3	1.122	3.115	.940	.924	.745	2.033	.890	.845
4	1.146	4.249	.989	.953	.761	2.786	.936	.885
5	1.159	5.401	.995	.970	.775	3.554	.944	.913
6	1.163	6.562	.995	.982	.787	4.335	.952	.945

Figure 8a. Dependence of the ratio of true to apparent surface tension on the ratio of surface to mean jet velocity: benzene, 2-butanol, ethanol and methanol

Figure 8b. Dependence of the ratio of true to apparent surface tension on the ratio of surface to mean jet velocity: water with varying velocities and orifices

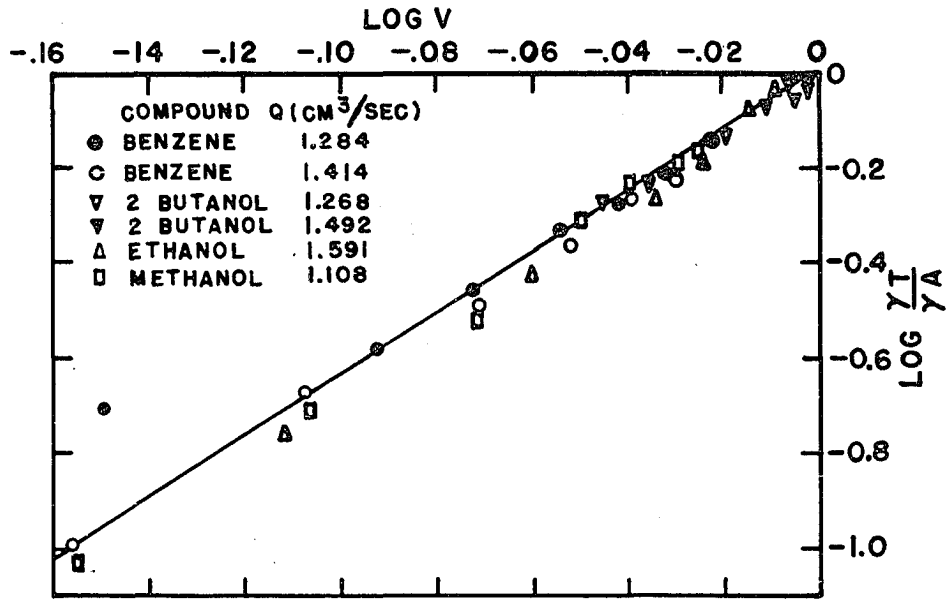
LOG V
-.16 -.14 -.12 -.10 -.08 -.06 -.04 -.02 0
0 -0.2 -0.4 -0.6 -0.8 -1.0
LOG γT/γA
COMPOUND Q(CM³/SEC)
BENZENE 1.284
BENZENE 1.414
2 BUTANOL 1.268
2 BUTANOL 1.492
ETHANOL 1.591
METHANOL 1.108

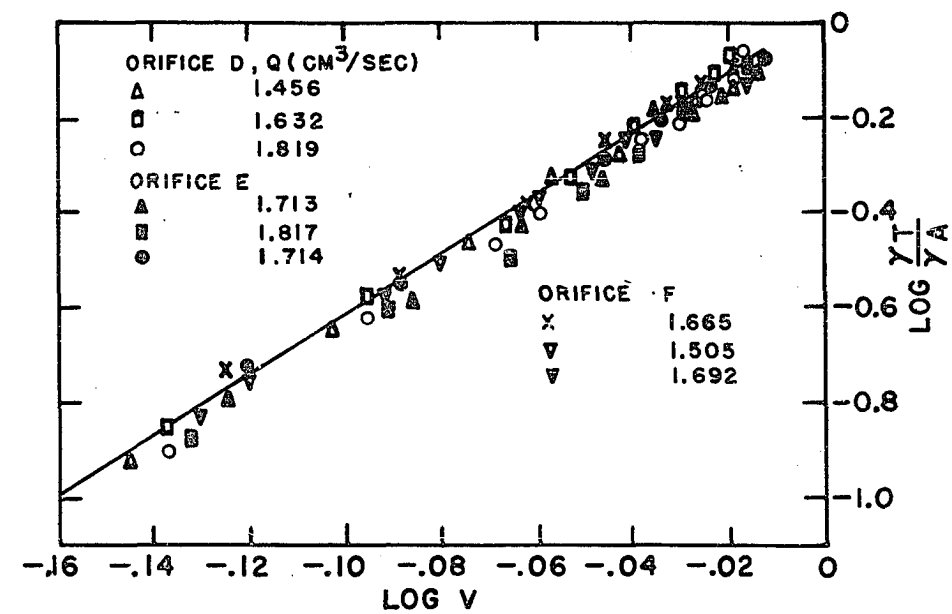
ORIFICE D, Q(CM³/SEC)
1.456
1.632
1.819
ORIFICE E
1.713
1.817
1.714
ORIFICE F
1.665
1.505
1.692
0 -0.2 -0.4 -0.6 -0.8 -1.0
LOG γT/γA
-.16 -.14 -.12 -.10 -.08 -.06 -.04 -.02 0
LOG V

Table 5

Dynamic surface tension of water: orifices D, E, and F

Orifice D Q=1.456 cm.^{3}/sec., T=20.1°C.					Orifice D Q=1.632 cm.^{3}/sec., T=20.6°C.			
n	λ (cm.)	z (cm.)	$\frac{\gamma_t}{\gamma_A}$	$\frac{V_s}{V_o}$	λ (cm.)	z (cm.)	$\frac{\gamma_t}{\gamma_A}$	$\frac{V_s}{V_o}$
1	.562	.706	.815	.714	.639	.857	.821	.729
2	.584	1.279	.865	.792	.667	1.510	.873	.800
3	.603	1.872	.904	.844	.684	2.186	.906	.857
4	.617	2.478	.932	.878	.699	2.877	.931	.886
5	.625	3.100	.941	.903	.711	3.576	.950	.909
6	.639	3.732	.969	.925	.721	4.283	.966	.928
7	.644	4.374	.971	.941	.730	5.013	.977	.944
8	.650	5.021	.973	.953	.733	5.745	.982	.954

Orifice D Q=1.819 cm.^{3}/sec., T=18.2°C.					Orifice E Q=1.505 cm.^{3}/sec., T=20.0°C.			
n	λ (cm.)	z (cm.)	$\frac{\gamma_t}{\gamma_A}$	$\frac{V_s}{V_o}$	λ (cm.)	z (cm.)	$\frac{\gamma_t}{\gamma_A}$	$\frac{V_s}{V_o}$
1	.716	.890	.812	.730	.584	.775	.814	.729
2	.744	1.570	.867	.800	.609	1.371	.867	.800
3	.762	2.323	.897	.854	.622	1.987	.889	.857
4	.781	3.094	.929	.889	.635	2.615	.915	.886
5	.792	3.881	.944	.914	.647	3.256	.933	.909
6	.799	4.676	.953	.933	.658	3.904	.954	.928

Table 5. (continued)

Orifice D Q=1.819 cm.^{3}/sec., T=18.2°C.					Orifice E Q=1.505 cm.^{3}/sec., T=20.0°C.			
n	λ (cm.)	z (cm.)	$\frac{\gamma_t}{\gamma_A}$	$\frac{V_s}{V_o}$	λ (cm.)	z (cm.)	$\frac{\gamma_t}{\gamma_A}$	$\frac{V_s}{V_o}$
7	.803	5.477	.962	.947	.660	4.561	.964	.944
8	.816	6.287	.973	.957	.673	5.236	.971	.954
9	.824	6.707	.984	.962	-	-	-	-

Orifice E Q=1.665 cm.^{3}/sec., T=21.1°C.					Orifice E Q=1.692 cm.^{3}/sec., T=18.5°C.			
n	λ (cm.)	z (cm.)	$\frac{\gamma_t}{\gamma_A}$	$\frac{V_s}{V_o}$	λ (cm.)	z (cm.)	$\frac{\gamma_t}{\gamma_A}$	$\frac{V_s}{V_o}$
1	.662	.918	.830	.752	.678	.919	.852	.756
2	.684	1.591	.873	.820	.695	1.605	.883	.818
3	.701	2.284	.902	.866	.709	2.307	.906	.878
4	.719	2.991	.922	.897	.728	3.026	.940	.901
5	.730	3.712	.956	.919	.736	3.758	.949	.923
6	.734	4.444	.956	.936	.743	4.497	.960	.939
7	.740	5.181	.959	.948	.754	5.246	.973	.951
8	.742	5.922	.912	.958	-	-	-	-

Table 5. (continued)

Orifice F Q=1.713 cm.^{3}/sec., T=20.2°C.					Orifice F Q=1.714 cm.^{3}/sec., T=19.8°C.			
n	λ (cm.)	z (cm.)	$\frac{\gamma_t}{\gamma_A}$	$\frac{V_s}{V_o}$	λ (cm.)	z (cm.)	$\frac{\gamma_t}{\gamma_A}$	$\frac{V_s}{V_o}$
1	.686	.904	.839	.742	.687	.905	.850	.750
2	.714	1.604	.893	.811	.708	1.603	.888	.816
3	.726	2.324	.911	.860	.724	2.319	.919	.866
4	.742	3.058	.938	.893	.741	3.051	.950	.898
5	.754	3.806	.955	.915	.754	3.799	.969	.921
6	.762	4.546	.969	.932	.762	4.557	.977	.937
7	.768	5.329	.971	.946	.767	5.321	.981	.951
8	-	-	-	-	.777	6.090	.986	.959

Orifice F Q=1.817 cm.^{3}/sec., T=19.5°C.				
n	λ (cm.)	z (cm.)	$\frac{\gamma_t}{\gamma_A}$	$\frac{V_s}{V_o}$
1	.732	1.040	.852	.761
2	.755	1.783	.893	.828
3	.773	2.547	.926	.873
4	.787	3.327	.947	.903
5	.799	4.120	.966	.925
6	.805	4.922	.970	.940

D. Dynamic Surface Tension

The dependence of the dynamic surface tension on time was measured for six solutions of heptanoic acid covering the concentration range from .00938 M/ls to .00750 M/ls. The measurements were made with orifice D, which had been "desicoted" at 20°C. The results are presented in Table 8 and Figure 11.

The dynamic surface tension as a function of time was measured for six solutions of 1-heptanol covering the concentration range from .00938 M/ls to .00750 M/ls. The measurements were made with orifice D, which had been "desicoted" at 20°C. The results are presented in Table 9 and Figure 12.

The relationships between surface tension and time for three solutions of octanoic acid in the concentration range from .00074 M/ls to .00150 M/ls were measured. Orifice D which had been "desicoted" was used at 20°C. The results are presented in Table 10 and Figure 13b.

The dependence of the dynamic surface tension on time was measured for pentanoic acid for the two concentrations .0075 M/ls and .0053 M/ls at 20°C. Orifice D was used and it had been "desicoted". The results are presented in Table 11 and Figure 13a.

At 10°C. the dynamic surface tensions dependence on time was measured with Orifice D over the concentration range from

.0015 M/ls to .00375 M/ls. The orifice had been previously "desicoted". The results are presented in Table 12 and Figure 14.

Table 6

Dynamic surface tension of pure water: dependence on time and temperature

n	λ (cm.)	z (cm.)	γ ($\frac{\text{dyne}}{\text{cm.}}$)	10^2t (sec.)	λ (cm.)	z (cm.)	γ ($\frac{\text{dyne}}{\text{cm.}}$)	10^2t (sec.)
	T=2.5°C., Q=1.596 cm.^{3}/sec.				T=5°C., Q=1.602 cm.^{3}/sec.			
1	.661	.809	77.8	.58	.615	.809	76.5	.58
2	.640	1.430	77.2	.91	.641	1.438	76.5	.91
3	.658	2.079	76.7	1.21	.664	2.091	75.4	1.21
4	.671	2.743	76.3	1.49	.676	2.761	75.6	1.50
5	.686	3.422	75.7	1.75	.689	3.443	74.9	1.76
6	.696	4.113	75.0	2.02	.703	4.135	74.4	2.00
	T=10°C., Q=1.630 cm.^{3}/sec.				T=12.5°C., Q=1.657 cm.^{3}/sec.			
1	.624	.813	76.7	.58	.635	.852	76.4	.60
2	.652	1.451	76.2	.90	.664	1.502	75.7	.92
3	.670	2.790	76.0	1.20	.684	2.176	74.9	1.22
4	.687	3.484	75.2	1.49	.703	2.869	73.8	1.52
5	.699	4.187	74.6	1.78	.710	3.576	74.0	1.82
6	.714	4.901	73.8	2.04	.722	4.292	74.1	2.10
7	.720	5.626	73.9	2.33	.734	5.020	73.9	2.38

Table 6. (continued)

	T=16.8°C., Q=1.680 cm.^{3}/sec.				T=20°C., Q=1.700 cm.^{3}/sec.			
n	λ (cm.)	z (cm.)	γ ($\frac{\text{dyne}}{\text{cm.}}$)	10^2t (sec.)	λ (cm.)	z (cm.)	γ ($\frac{\text{dyne}}{\text{cm.}}$)	10^2t (sec.)
1	.649	.874	74.6	.62	.652	.871	73.3	.62
2	.676	1.537	74.3	.94	.681	1.537	72.8	.96
3	.699	2.124	73.2	1.20	.699	2.222	72.9	1.26
4	.712	2.830	73.3	1.50	.715	2.924	72.5	1.54
5	.724	3.548	73.2	1.80	.732	3.648	72.7	1.84
6	.730	4.275	73.4	2.08	.736	4.383	72.6	2.12
7	-	-	-	-	.741	5.123	72.7	2.40

Figure 9. Effect of temperature on the rate of attainment of equilibrium surface tension of water

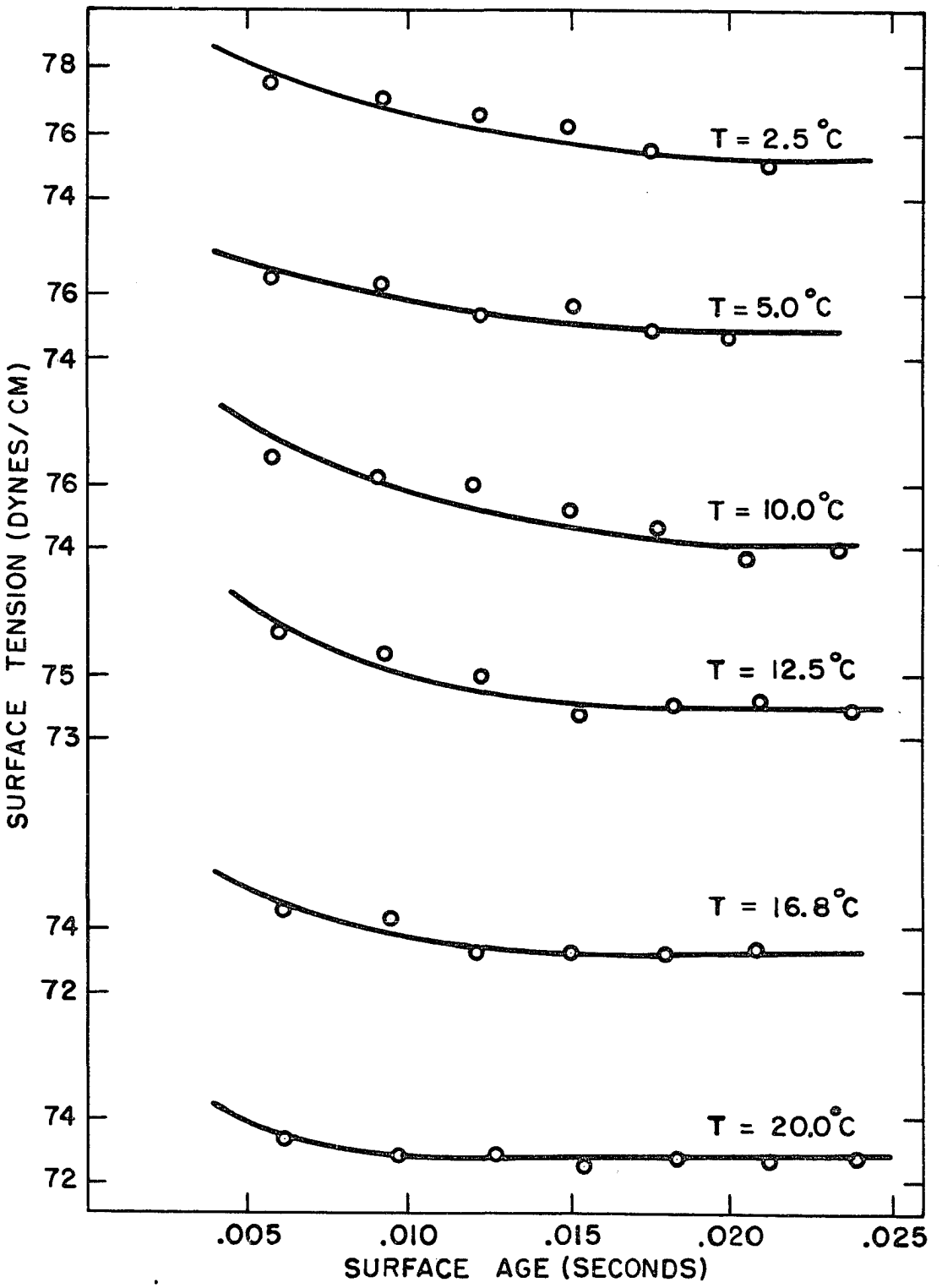
78
76
74
T = 2.5 °C
76
74
T = 5.0 °C
76
74
T = 10.0 °C
75
73
T = 12.5 °C
74
72
T = 16.8 °C
74
72
T = 20.0 °C
SURFACE TENSION (DYNES/CM)
.005
.010
.015
.020
.025
SURFACE AGE (SECONDS)

Table 7

Dynamic surface tensions: heptanoic acid solutions for orifices E and F

Q=1.723 cm.^{3}/sec.

	.0015 M/ls	Orifice E			.00188 M/ls			
n	λ (cm.)	z (cm.)	γ ($\frac{\text{dyne}}{\text{cm.}}$)	10^2t (sec.)	λ (cm.)	z (cm.)	γ ($\frac{\text{dyne}}{\text{cm.}}$)	10^2t (sec.)
1	.679	.947	72.1	.64	.682	.893	68.9	.61
2	.711	1.642	70.6	.96	.722	1.595	66.6	.95
3	.735	2.365	69.7	1.28	.751	2.336	65.1	1.26
4	.755	3.110	68.6	1.59	.779	3.096	63.4	1.58
5	.775	3.875	67.0	1.90	.795	3.879	62.6	1.90
6	.790	4.658	66.1	2.10	.806	4.674	62.0	2.20
7	.797	5.451	65.8	2.49	-	-	-	-

Q=1.713 cm.^{3}/sec.

	.001883 M/ls	Orifice F			.0025 M/ls			
n	λ (cm.)	z (cm.)	γ ($\frac{\text{dyne}}{\text{cm.}}$)	10^2t (sec.)	λ (cm.)	z (cm.)	γ ($\frac{\text{dyne}}{\text{cm.}}$)	10^2t (sec.)
1	.695	.926	67.9	.63	.733	.940	66.1	.63
2	.729	1.638	66.8	.92	.776	1.664	63.1	.92
3	.760	2.383	65.1	1.29	.802	2.423	62.7	1.29
4	.787	3.156	63.1	1.60	.832	3.210	60.2	1.62
5	.802	3.956	62.3	1.92	.848	4.020	59.7	1.94
6	.818	4.771	61.7	2.25	.874	4.848	59.1	2.27

Table 7. (continued)

		Q=1.713 cm.^{3}/sec.		
		.0075 M/ls		Orifice F
n	λ (cm.)	z (cm.)	γ ($\frac{\text{dyne}}{\text{cm.}}$)	10^2t (sec.)
1	.860	1.091	47.3	.70
2	.909	1.980	45.6	1.12
3	.943	2.908	44.7	1.50
4	.965	3.862	44.3	1.88
5	.985	4.836	43.6	2.36
6	1.000	5.828	43.4	2.63

Table 8

Dynamic surface tension: heptanoic acid
(Q=1.690 cm.^{3}/sec.)

	.000938 M/ls				.00150 M/ls			
n	λ (cm.)	z (cm.)	γ ($\frac{\text{dyne}}{\text{cm.}}$)	10^2t (sec.)	λ (cm.)	z (cm.)	γ ($\frac{\text{dyne}}{\text{cm.}}$)	10^2t (sec.)
1	.659	.905	73.1	.63	.659	.899	71.4	.63
2	.688	1.579	72.6	.99	.686	1.572	71.0	.97
3	.711	2.278	71.8	1.29	.714	2.272	69.5	1.29
4	.728	2.998	71.2	1.58	.736	2.997	68.0	1.58
5	.739	3.731	71.3	1.87	.758	3.744	67.2	1.88
6	.747	4.479	71.5	2.17	.769	4.507	66.2	2.17
7	.763	5.239	70.2	2.45	.780	5.282	65.8	2.46
8	.775	6.008	69.3	2.73	-	-	-	-
	.00188 M/ls				.00250 M/ls			
n	λ (cm.)	z (cm.)	γ ($\frac{\text{dyne}}{\text{cm.}}$)	10^2t (sec.)	λ (cm.)	z (cm.)	γ ($\frac{\text{dyne}}{\text{cm.}}$)	10^2t (sec.)
1	.661	.830	70.5	.58	.700	.899	66.3	.65
2	.705	1.513	67.9	.95	.747	1.623	63.1	1.01
3	.737	2.234	65.9	1.27	.778	2.386	61.8	1.36
4	.762	2.984	64.1	1.58	.803	3.177	59.2	1.66
5	.785	3.757	62.1	1.88	.823	3.993	59.6	1.97
6	.803	4.551	61.5	2.18	.843	4.830	57.9	2.29

Table 8. (continued)

n	.00375 M/ls				.0075 M/ls			
	λ (cm.)	z (cm.)	γ ($\frac{\text{dyne}}{\text{cm.}}$)	10^2t (sec.)	λ (cm.)	z (cm.)	γ ($\frac{\text{dyne}}{\text{cm.}}$)	10^2t (sec.)
1	.743	.984	59.7	.68	.846	1.140	47.3	.73
2	.786	1.749	57.8	1.08	.885	2.005	46.3	1.18
3	.822	2.553	55.9	1.41	.924	2.910	45.3	1.54
4	.851	3.389	54.2	1.75	.948	3.846	44.6	1.90
5	.874	4.252	53.1	2.07	.977	4.809	43.9	2.28
6	.886	5.132	53.1	2.39	.994	5.795	43.9	2.65

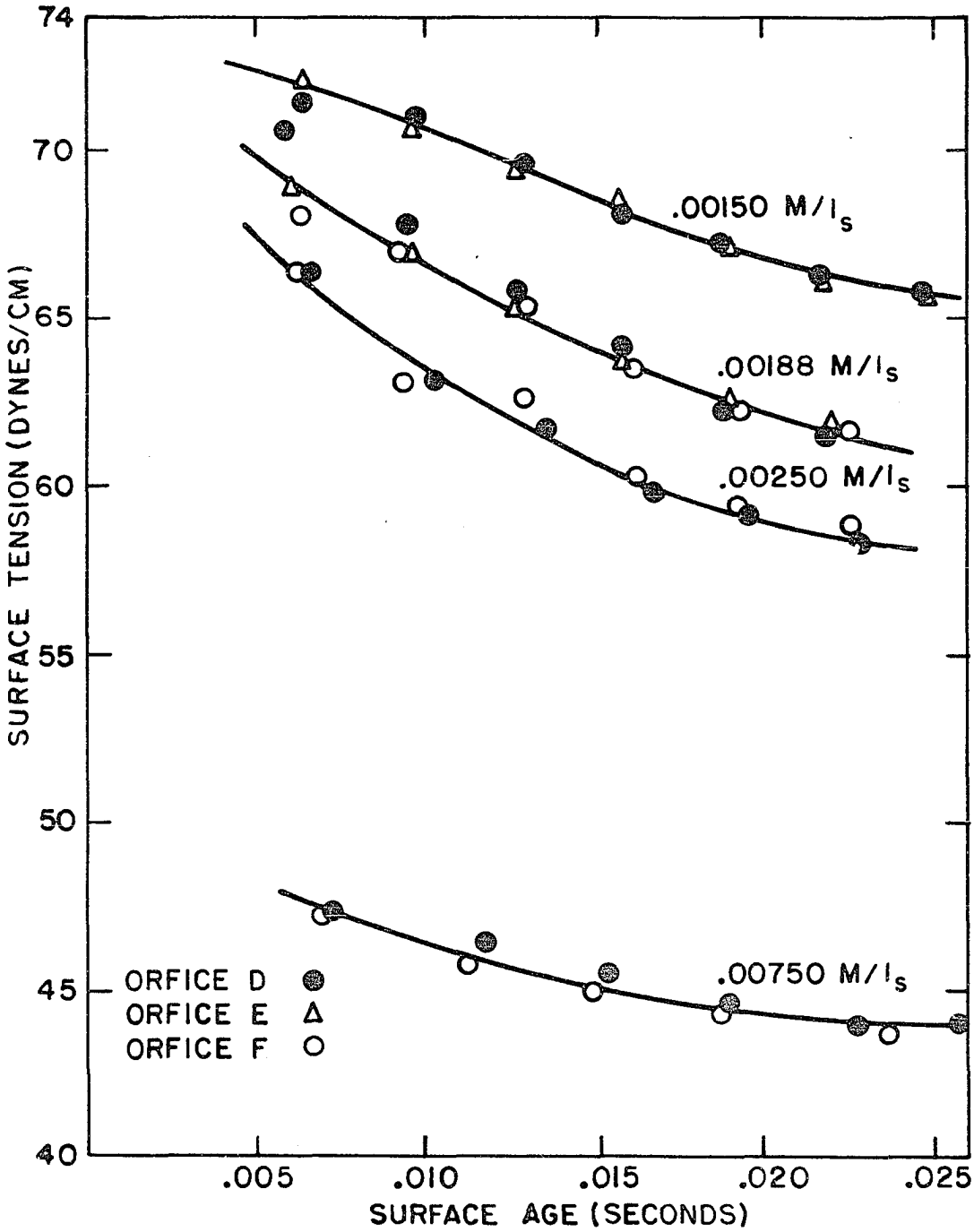

Figure 10. Comparison of the dynamic surface tension for different orifices at a given concentration

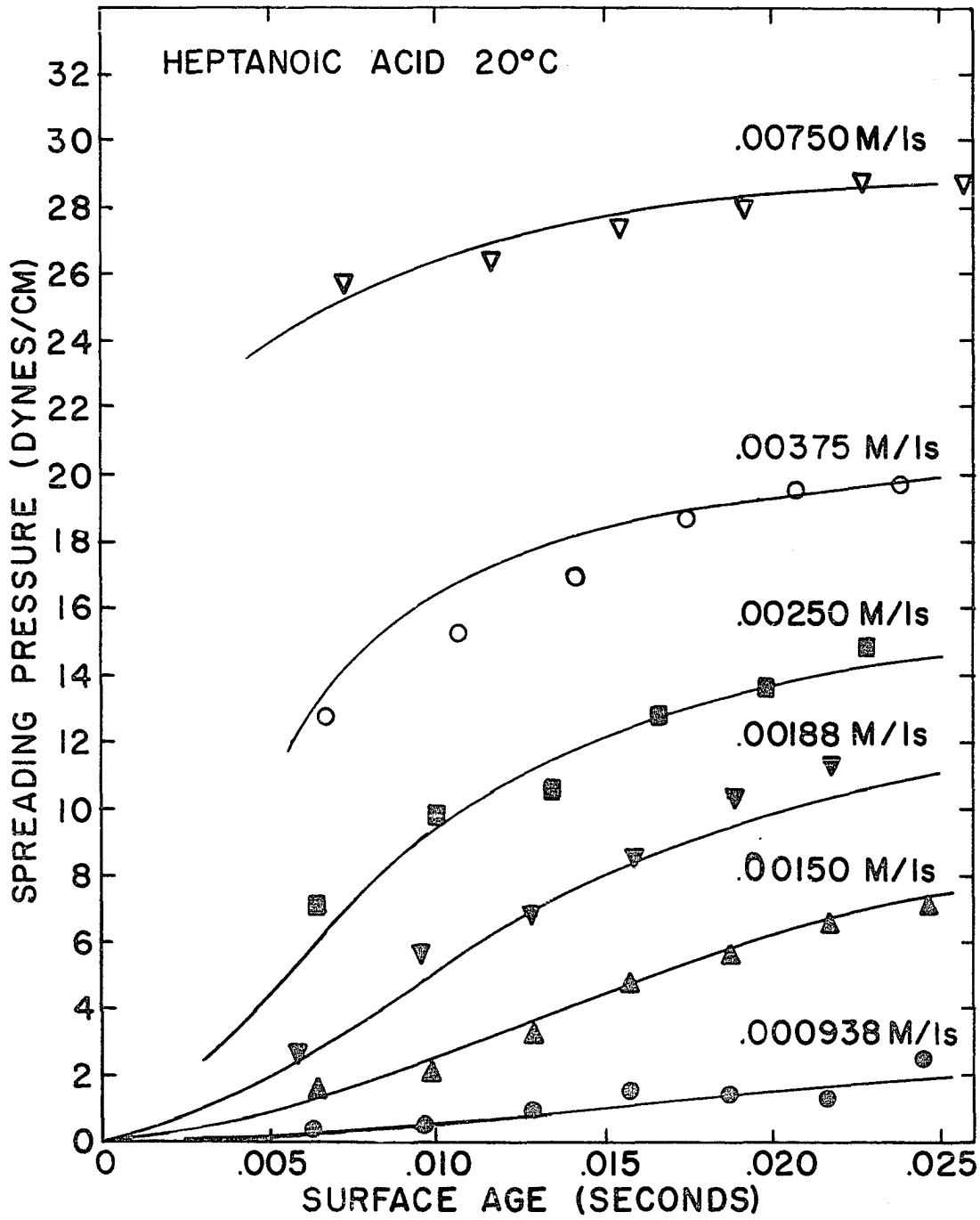

Figure 11. Comparison of experimental points with theoretical equation 16: heptanoic acid 20°C.

Table 9

Dynamic surface tension: 1-heptanol solutions at 20°C.
(Q=1.685 cm.^{3}/sec.)

n	.00938 M/ls				.00150 M/ls			
	λ (cm.)	z (cm.)	γ ($\frac{\text{dyne}}{\text{cm.}}$)	10^2t (sec.)	λ (cm.)	z (cm.)	γ ($\frac{\text{dyne}}{\text{cm.}}$)	10^2t (sec.)
1	.650	.831	72.8	.58	.660	.859	72.0	.61
2	.685	1.493	71.5	.94	.700	1.540	68.8	.96
3	.703	2.189	71.7	1.26	.726	2.261	68.5	1.29
4	.719	2.901	71.3	1.55	.750	2.999	66.7	1.58
5	.744	3.633	70.8	1.83	.775	3.774	64.9	1.89
6	.745	4.357	70.7	2.11	.794	4.553	63.5	2.18
7	.754	5.112	70.4	2.41	.805	5.351	63.3	2.49
8	.766	5.881	70.0	2.70	-	-	-	-

n	.00188 M/ls				.00250 M/ls			
	λ (cm.)	z (cm.)	γ ($\frac{\text{dyne}}{\text{cm.}}$)	10^2t (sec.)	λ (cm.)	z (cm.)	γ ($\frac{\text{dyne}}{\text{cm.}}$)	10^2t (sec.)
1	.659	.840	71.5	.60	.705	.901	64.8	.63
2	.709	1.520	68.8	.96	.757	1.632	61.3	1.00
3	.746	2.249	64.6	1.29	.787	2.444	60.0	1.34
4	.772	3.008	63.0	1.58	.819	3.198	57.8	1.67
5	.793	3.795	61.6	1.89	.836	4.028	57.4	1.94
6	.812	4.592	60.5	2.19	.856	4.871	56.2	2.31
7	.827	5.413	59.8	2.51	-	-	-	-

Table 9. (continued)

	.00375 M/ls				.0075 M/ls			
n	λ (cm.)	z (cm.)	γ ($\frac{\text{dyne}}{\text{cm.}}$)	10^2t (sec.)	λ (cm.)	z (cm.)	γ ($\frac{\text{dyne}}{\text{cm.}}$)	10^2t (sec.)
1	.753	.959	58.3	.66	.874	1.111	44.0	.74
2	.804	1.741	56.0	1.05	.928	2.012	42.5	1.17
3	.845	2.570	53.2	1.41	.964	2.961	41.7	1.57
4	.871	3.432	52.1	1.75	.999	3.940	40.4	1.95
5	.895	4.355	51.1	2.11	1.019	4.947	40.2	2.34
6	.912	5.312	50.8	2.48	1.037	5.986	40.1	2.74

Figure 12. Comparison of experimental points with equation 16: 1-heptanol solutions

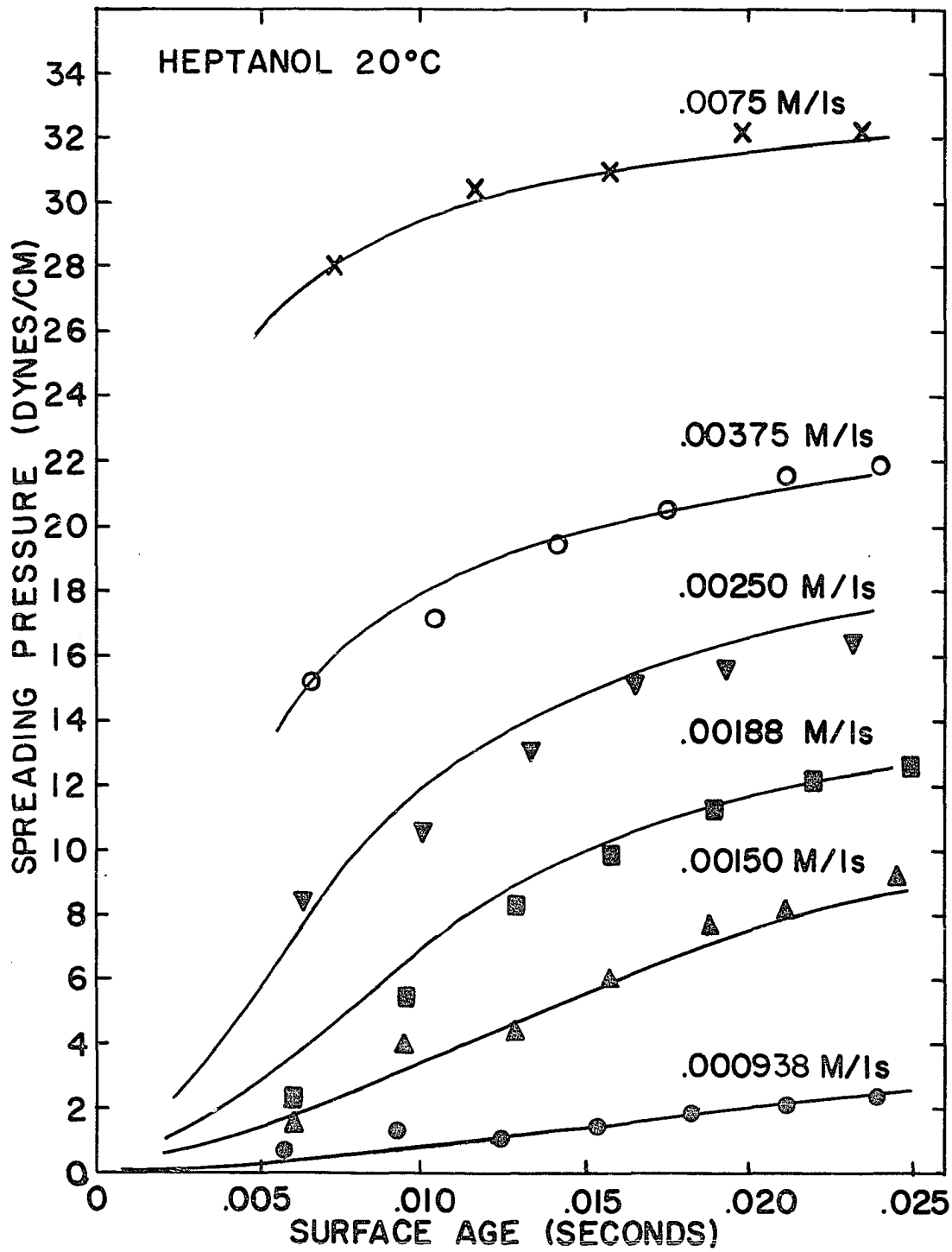
HEPTANOL 20°C
.0075 M/ls
.00375 M/ls
.00250 M/ls
.00188 M/ls
.00150 M/ls
.000938 M/ls
SPREADING PRESSURE (DYNES/CM)
SURFACE AGE (SECONDS)
0
2
4
6
8
10
12
14
16
18
20
22
24
26
28
30
32
34
.005
.010
.015
.020
.025

Table 10

Dynamic surface tension: octanoic acid solutions
($Q=1.691$ cm.^{3}/sec.)

	.0074 M/ls				.0011 M/ls			
n	λ (cm.)	z (cm.)	γ ($\frac{\text{dyne}}{\text{cm.}}$)	10^2t (sec.)	λ (cm.)	z (cm.)	γ ($\frac{\text{dyne}}{\text{cm.}}$)	10^2t (sec.)
1	.657	.889	73.0	.62	.661	.891	72.8	.62
2	.689	1.562	72.6	.97	.692	1.564	72.0	.97
3	.711	2.262	72.1	1.29	.719	2.265	20.6	1.29
4	.725	2.980	71.9	1.58	.742	2.996	68.8	1.58
5	.739	3.712	71.4	1.86	.764	3.749	67.2	1.88
6	.748	4.456	71.3	2.11	.780	4.521	66.1	2.13

	.0014 M/ls			
n	λ (cm.)	z (cm.)	γ ($\frac{\text{dyne}}{\text{cm.}}$)	10^2t (sec.)
1	.663	.821	72.0	.62
2	.703	1.573	70.0	1.00
3	.740	2.298	65.6	1.30
4	.770	3.056	64.4	1.59
5	.779	3.840	61.9	1.90
6	.821	4.650	60.2	2.15

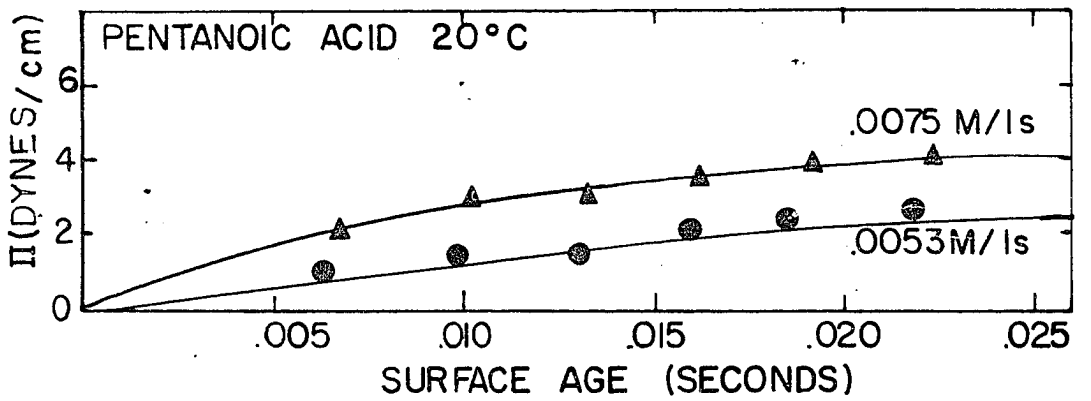

Figure 13a. Comparison of experimental points with equation 16: valeric acid solutions

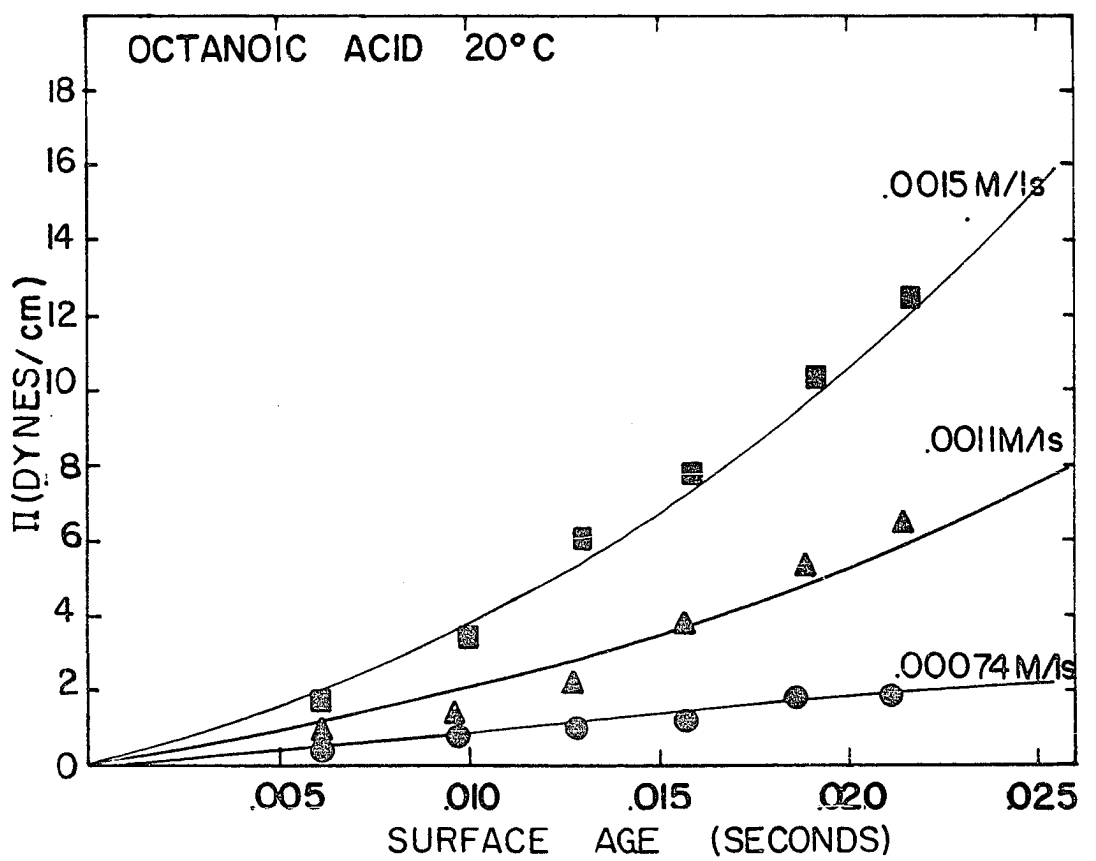

Figure 13b. Comparison of experimental points with equation 16: octanoic acid solutions

Table 11

Dynamic surface tension: pentanoic acid solutions
($Q=1.710$ cm.^{3}/sec.)

	.0053 M/ls				.0075 M/ls			
n	λ (cm.)	z (cm.)	γ ($\frac{\text{dyne}}{\text{cm.}}$)	10^2t (sec.)	λ (cm.)	z (cm.)	γ ($\frac{\text{dyne}}{\text{cm.}}$)	10^2t (sec.)
1	.673	.909	72.4	.63	.681	.952	71.4	.67
2	.703	1.597	71.6	.99	.712	1.649	70.2	1.02
3	.724	2.311	71.3	1.31	.734	2.372	70.0	1.34
4	.740	3.043	70.7	1.60	.748	3.113	69.5	1.63
5	.751	3.788	70.1	1.84	.760	3.867	69.4	1.93
6	.761	4.544	70.1	2.19	.774	4.634	69.0	2.22

Table 12

Dynamic surface tension: heptanoic acid at 10°C.
($Q=1.635$ cm.^{3}/sec.)

n	.0015 M/ls				.00188 M/ls			
	λ (cm.)	z (cm.)	γ ($\frac{\text{dyne}}{\text{cm.}}$)	10^2t (sec.)	λ (cm.)	z (cm.)	γ ($\frac{\text{dyne}}{\text{cm.}}$)	10^2t (sec.)
1	.632	.828	75.1	.59	.634	.815	74.1	.59
2	.665	1.480	73.5	.91	.676	1.572	72.2	.96
3	.691	2.159	72.0	1.22	.707	2.263	69.5	1.26
4	.710	2.860	70.7	1.52	.727	2.980	68.2	1.57
5	.728	3.579	69.5	1.81	.748	3.718	66.6	1.87
6	.744	4.315	68.3	2.11	.767	4.475	64.9	2.17
7	.755	5.059	68.0	2.40	.783	5.250	63.6	2.47

n	.00250 M/ls				.00375 M/ls			
	λ (cm.)	z (cm.)	γ ($\frac{\text{dyne}}{\text{cm.}}$)	10^2t (sec.)	λ (cm.)	z (cm.)	γ ($\frac{\text{dyne}}{\text{cm.}}$)	10^2t (sec.)
1	.651	.827	71.9	.59	.709	.925	61.0	.65
2	.702	1.509	67.2	.92	.752	1.656	59.9	1.00
3	.738	2.223	64.8	1.24	.783	2.422	57.9	1.30
4	.765	2.982	62.7	1.56	.810	3.216	56.4	1.67
5	.787	3.765	61.0	1.88	.827	4.036	55.9	2.00
6	.799	4.558	60.8	2.19	.852	4.885	53.9	2.32

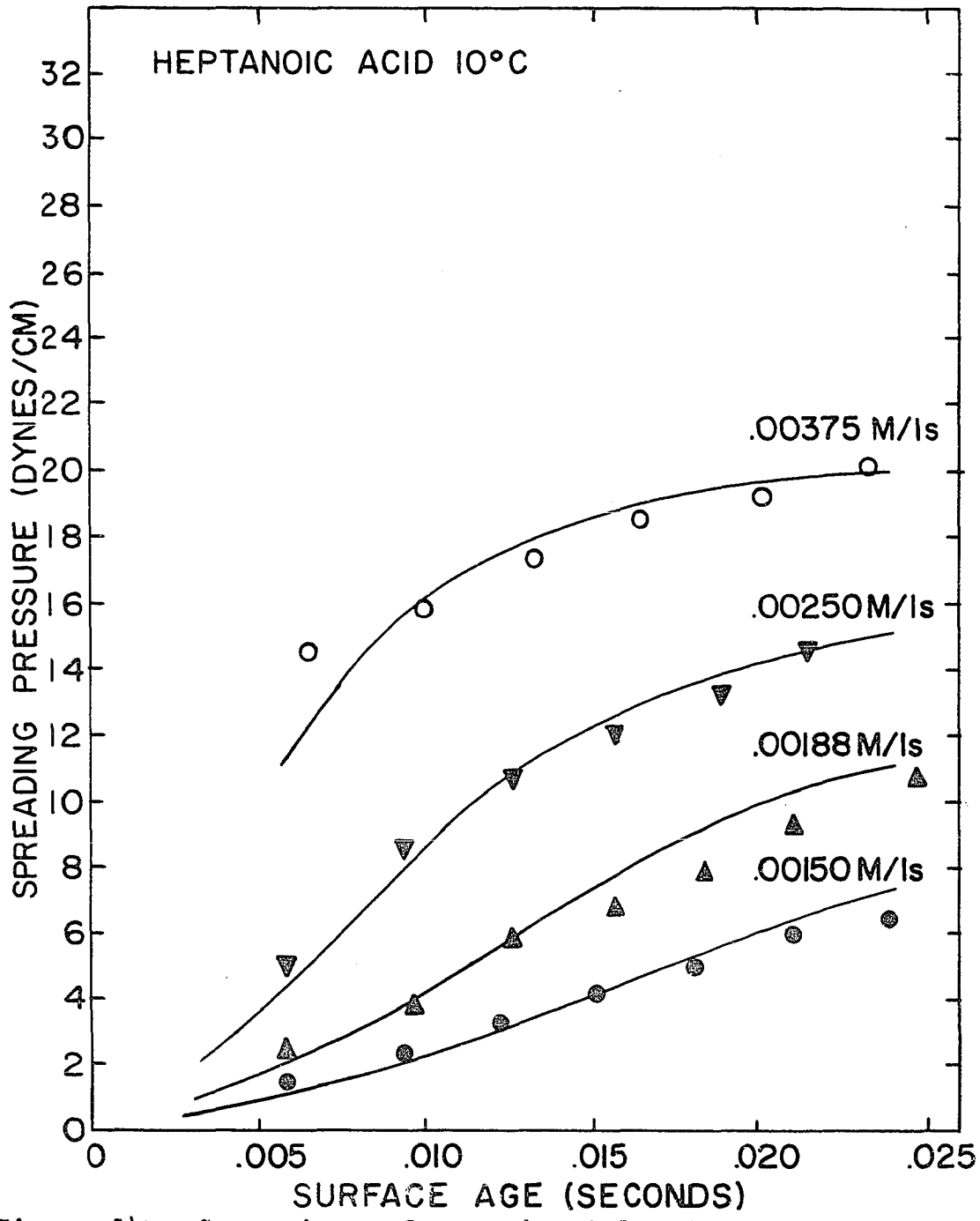

Figure 14. Comparison of experimental points with equation 16: heptanoic acid solutions 10°C.

VI. DISCUSSION AND THEORY

A. Verification of n

From Figure 8a and Figure 8b it is apparent that the work done here agrees with that of Hansen, Purchase, Wallace and Woody (25). Not only does the value of n obtained here ($n = .645 \pm .013$) agree with their value ($n = .63 \pm .01$), but the result is further evidence of the independence of the method on the orifice used. The orifices used in their work were made of pyrex as here, but they were not treated with Beckman "Desicote". These two sets of orifices with entirely different surface characteristics (i.e., the "desicoted" orifices were water repellant whereas the other orifices were wet by the water) gave mutually consistent results.

B. Independence of the Dynamic Surface Tension on Orifice

The results shown in Figure 10 indicate that the dynamic surface tension-time curves are independent of the orifice used. Of course, the reservation must be made that the orifices must conform to the design given earlier. This result is a contradiction of the conclusions of Rideal and Sutherland (41). Their dynamic surface tension-time curves corresponding to the two different orifices used were displaced along the time axes from each other by as much as 40 per cent. The greatest

deviation in the curves obtained here was the scatter of the data corresponding to the first wave length. All of the other experimental points agreed within experimental error.

It is interesting to note that in the work of Posner and Alexander (35, p. 657) two different types of orifices were used. One was similar in design to the bell shaped orifices of Rideal and Sutherland; the other was similar in design to the orifices used in this work. The bell shaped orifice gave results that were dependent on the discharge rate (they evidently considered this difference to be within experimental error). The orifice similar to those used here gave results which were independent of the discharge rate.

It is almost impossible to compare the existing data obtained in different laboratories by the vibrating jet method. First of all, the different orifice designs (i.e., bell shaped, thin plate, etc.) make it impossible to apply the corrections for non-uniform velocity profile and true surface age which were developed by Hansen, Purchase, Wallace and Woody. This is because of lack of sufficient data on the dimensions of the orifices. Secondly, if the information were available, it appears that the theory of Hansen, Purchase, Wallace and Woody would be insufficient to treat the bell shaped orifices.

C. Semi-empirical Correlation of the Dynamic Surface Tension-Time Curves

In the course of interpretating the data obtained in this

work it appeared that two functional groups ($\frac{\pi}{\pi_\infty}$, $\pi_\infty^2 t$, where π is the spreading pressure at time t and π_∞ is the spreading pressure at infinite time) reduced the experimental data to a family of curves dependent only upon the length of the hydrocarbon tail of the fatty acid molecule. Figure 15 is characteristic of the curves obtained by plotting $\pi_\infty^2 t$ versus π/π_∞. The spreading pressure is defined as the difference between the dynamic surface tension of water at time t and the dynamic surface tension of the surface active solution at time t. From this it is clear that the equilibrium spreading pressure is the difference between the static surface tension of pure water and the static surface tension of a given concentration. Table 13 lists the equilibrium spreading pressures of the compounds used in this study.

It should be noted that the dynamic surface tension of water at 20°C. is constant within experimental error over the time range measured except for possibly the first wave length. A correction was found from an extrapolation of the dynamic surface tension of water at other temperatures for the first wave length. This correction is described in the next section.

The character of the curve obtained by plotting $u = \pi/\pi_\infty$ versus $\pi_\infty^2 t$ suggests that the data may be fit by a two parameter equation of the form

$$\frac{u}{1-u} \exp(-bu) = k \pi_\infty^2 t \qquad (16)$$

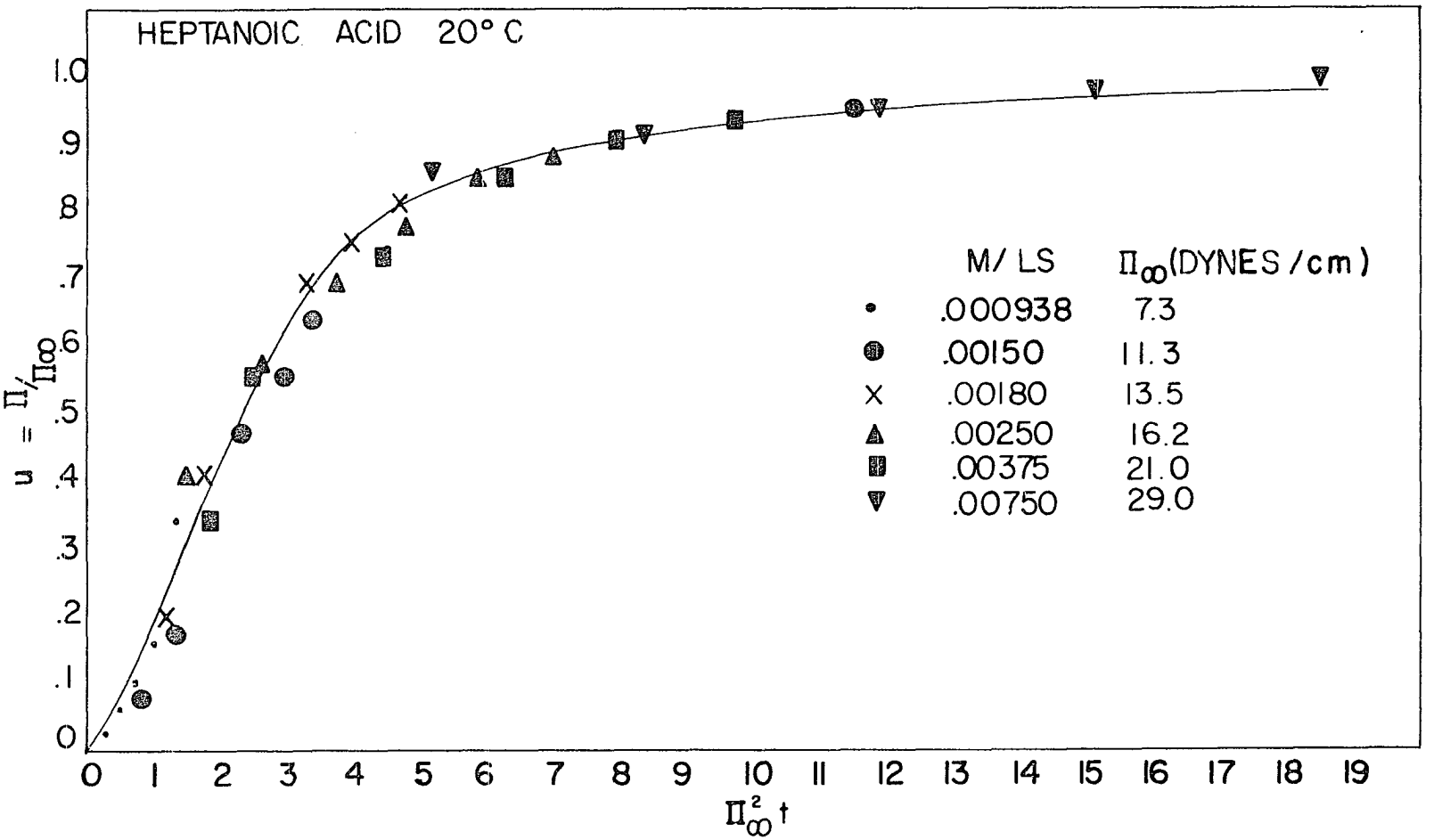

Figure 15. Characteristic reduced plot of experimental data

where the constants b and k are characteristic of the particular compound. Table 14 lists the constants needed to fit the experimental data. Figure 11 through Figure 14 compares the fit of the experimental points with equation 16.

From these results it is apparent that equation 16 represents the data exceptionally well. The largest deviation occurs for small spreading pressures.

To further justify the independence of the data obtained by the vibrating jet method on the orifice used, it is necessary that the results be compared with dynamic surface tension-time data obtained by other methods.

Addison (5) has measured the rate of surface tension depression for decanoic acid at 20°C. with the drop weight method (33) using the corrections of Harkins and Brown (27). He estimated the accuracy of the time to be ± 1 second and the surface tension to be accurate to a few per cent. When a plot of u versus $\pi_{\infty}{}^{2}t$ was made, the same characteristic curve as shown in Figure 16 was obtained. Figure 16 compares the experimental points of Addison with equation 16. Table 14 lists the constants b and k.

Dervichian (17) has measured the rate of surface tension depression for hendecanoic acid at 20°C. with the Wilhelmy-plate method (33). He did not make any estimate of error, but it seems safe to assume that the error would be of the same order as that of Addison. Again a plot of u versus $\pi_{\infty}{}^{2}t$ gave the characteristic curve. Figure 17 compares the experi-

Table 13

Equilibrium spreading pressures

Heptanoic Acid[a] 20°C.		1-Heptanol[b] 20°C.		Heptanoic Acid[c] 10°C.	
Conc. (M/ls)	π_∞ (dynes/cm.)	Conc. (M/ls)	π_∞ (dynes/cm.)	Conc. (M/ls)	π_∞ (dynes/cm.)
.000938	7.3	.000938	8.5	.00150	12.2
.00150	11.3	.00150	12.7	.00188	14.3
.00188	13.5	.00188	15.5	.00250	17.0
.00250	16.2	.00250	18.7	.00375	21.8
.00375	21.0	.00375	23.3		
.00750	29.0	.00750	32.8		

Octanoic Acid[d] 20°C.		Pentanoic Acid[e] 20°C.	
Conc. (M/ls)	π_∞ (dynes/cm.)	Conc. (M/ls)	π_∞ (dynes/cm.)
.00074	17.5	.0053	2.8
.0011	23.3	.0075	4.3
.0014	27.5		

[a]Average of the data of King (29) and Weber and Sternganz (53).

[b]Taken from the data of Posner, Anderson, and Alexander (37).

[c]Data from (29) and (53) was corrected for temperature using (28).

[d]Data of Frumkin (20) corrected for temperature.

[e]Data of King (29).

Table 14

Experimental constants

Compounds	b[a]	k[b]	x_o[c]	f_o[d]
Pentanoic Acid	1.12	2.62	5.96×10^{-3}	4.60×10^{3}
Heptanoic Acid (20°C.)	1.04	1.35×10^{-1}	3.35×10^{-4}	5.51×10^{4}
Octanoic Acid	1.14	1.50×10^{-2}	9.50×10^{-5}	1.84×10^{4}
Decanoic Acid	0.80	1.91×10^{-4}	6.07×10^{-6}	2.09×10^{6}
Hendecanoic Acid	1.07	7.80×10^{-6}	1.71×10^{-6}	7.06×10^{7}
1-Heptanol	0.93	1.28×10^{-1}	2.68×10^{-4}	6.05×10^{4}
Heptanoic Acid (10°C.)	1.06	1.00×10^{-1}	2.97×10^{-4}	5.40×10^{4}

[a]The constant b is dimensionless.

[b]The constant k has the dimensions $cm.^2/dyne^2\text{-}sec.$

[c]x_o is the solubility expressed in mole fractions. The data listed here is taken from (18) and (39).

[d]f_o is Traube's constant and has the dimensions dyne/cm.-M/ls. These values were obtained from the constants B and a listed by Addison (4, 5) for the equation $\pi = B\sigma_o \log_{10}(1 + c/a)$. By definition $f_o = \lim. \pi/c$, one obtains $f_o = 2.303\ B\ \sigma_o/a$, where σ_o is the surface tension of water.

mental points of Dervichian with equation 16. Table 14 lists the constants b and k.

The success of equation 16 in correlating the data of a fairly large range of fatty acids obtained by three different methods is encouraging. The question arises as to whether the data obtained by the drop weight method and the Wilhelmy-plate method group differently than those data obtained by the vibrating jet method. From Table 14 it is apparent that the constant b is independent of the compound studied and is approximately equal to one. The constant k appears to have a regular trend which depends on the length of the fatty acid molecule. It might be expected that the rate at which the fatty acid molecules are adsorbed into the surface would depend on the number of molecules in the bulk solution. A relative measure of the number of molecules in bulk solution is the solubility. Consequently it is to be expected that a plot of log k versus log x_o (where x_o is the solubility expressed in mole fractions) should yield a continuous curve. Figure 18 is such a plot. The linear relationship obtained is further verification of the independence of the data obtained by the vibrating jet method of the experimental design of the apparatus.

It was not possible to carry the analysis of equation 16 any further. Though it is successful in correlating a wide range of data, it has not proven susceptible to mechanistic

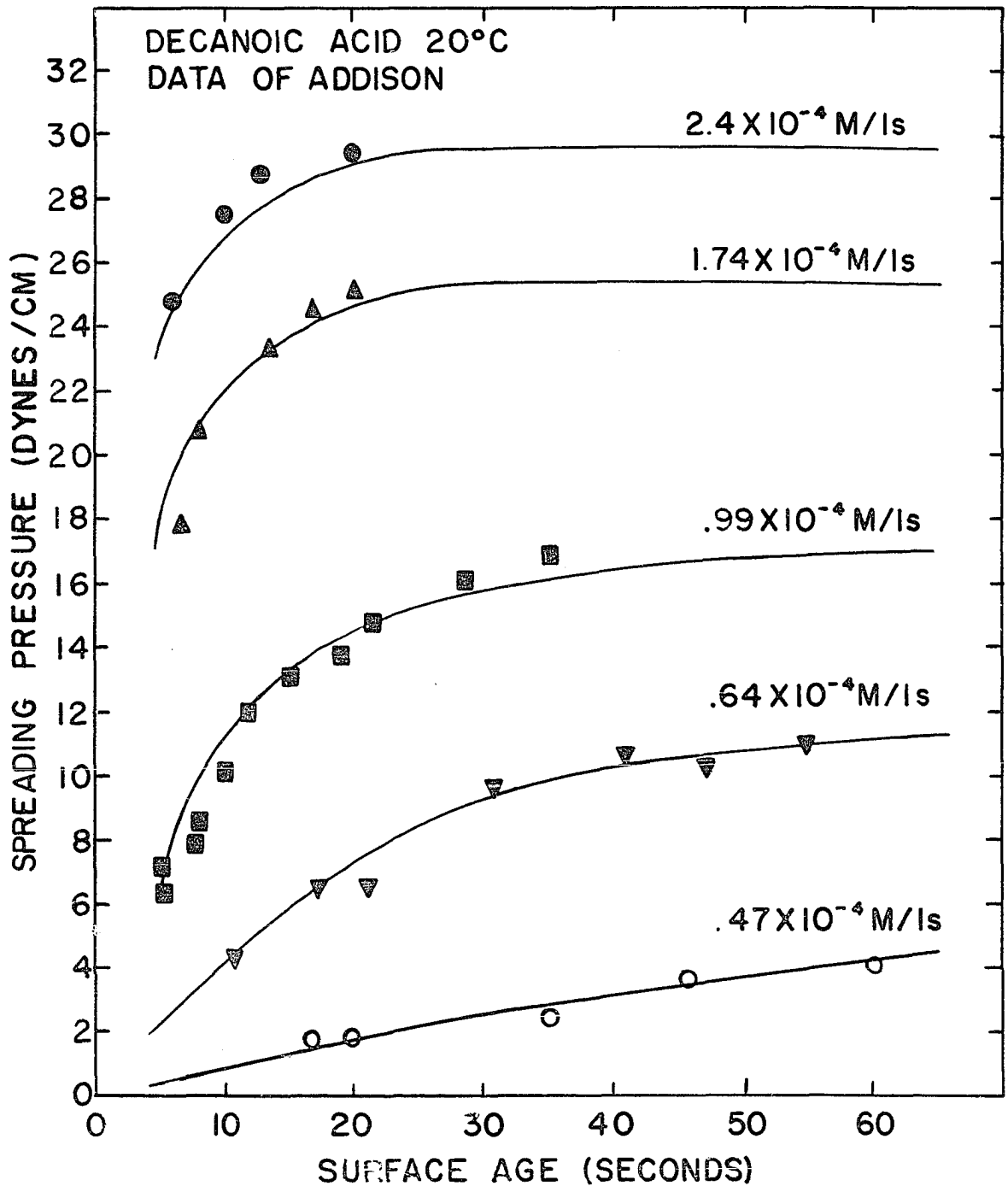

Figure 16. Comparison of experimental points with equation 16

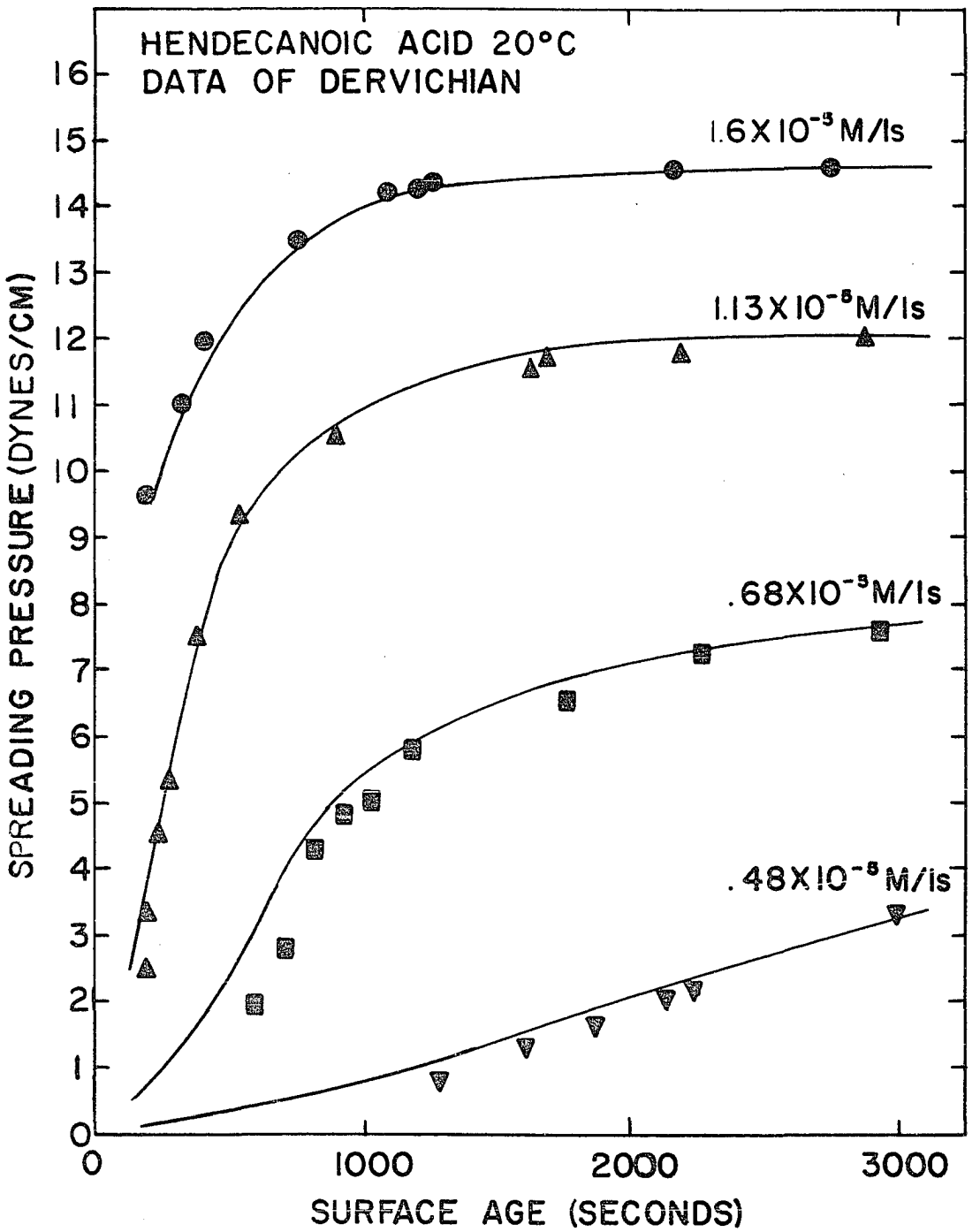

Figure 17. Comparison of experimental points with equation 16

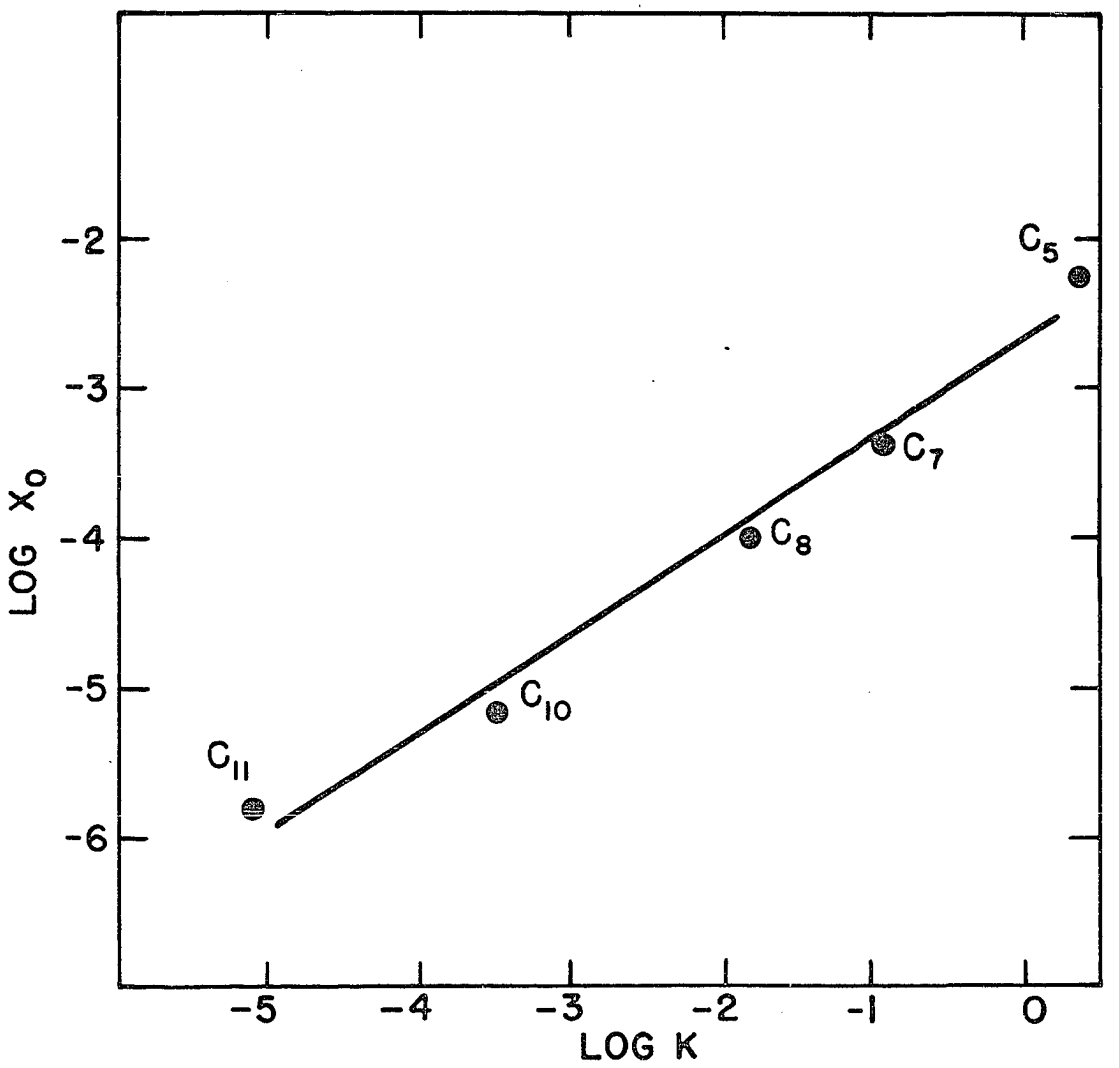

Figure 18. Relation between log X_o and log K

interpretation.

Since the 1-heptanol data was represented with approximately the same constants as the heptanoic acid it would appear that it is adsorbed by the same mechanism.

Before going on to the more general theory it would be best to view the interesting results obtained with pure water.

D. Dynamic Surface Tension of Water

Previous workers (1, 8) using the vibrating jet method have concluded that their results gave no evidence of a reorientation at the fresh liquid surface (i.e., no change of surface tension with time) after .001 seconds. Their experiments were carried out in the neighborhood of 20°C. The surface age was not corrected nor were any corrections made for velocity profile on the surface tension. It is felt that these workers overlooked the orientation effect because of a failure to make measurements as a function of temperature. Generally the relaxation time in bulk water, 10^{-10} sec. (47), is cited as evidence that reorientation would occur too rapidly to be measured.

When runs were made in this work at 20°C. or higher it appeared that the surface tension of water was independent of time within experimental error. At 2.5°C., however, a significant lowering of surface tension was observed over the observable time period. From Figure 9 it is apparent that

there is a definite trend toward an increasing length of time needed to reach the equilibrium surface tension.

Schmidt and Steyer (44) have observed the same qualitative trend for water. In their experiment, they passed a powerful air current over the open end of a capillary which extended into a container of water. The difference in pressure raised water to the top of the tube where it was atomized into spray. By stopping the air current at a definite time, the liquid rapidly sank to the position determined by surface tension. The position which the meniscus occupied at very short intervals of time after stopping the air current was determined. They then compared the rate of fall with that of an ideal falling liquid. They observed a lag in the rate of fall for water. For other liquids such as benzene and nitrobenzene this lag was not observed. They were able to fit their data with an empirical equation of the form

$$\frac{\gamma_{(t)} - \gamma_{\infty}}{\gamma_{o} - \gamma_{\infty}} = \exp(-\alpha t) \qquad (17)$$

where γ_{∞} is the equilibrium surface tension of water, $\gamma_{(t)}$ is the dynamic surface tension of water at time t and γ_{o} is the extrapolated value of the surface tension at zero time. The constant α in their equation decreased with a decrease of temperature until a minimum was reached around 13°C. There was a slight increase with further decrease of temperature. They obtained a maximum value of γ_{o} of 97 dyne/cm. at 13°C. They gave no explanation for the over all behavior.

In this work there was no apparent minimum value of α and the values of α obtained here were an order of magnitude smaller than those of Schmidt and Steyer. The extrapolated values of γ_o found here were in the neighborhood of 83 ± 3 dynes/cm. The experimental error was of such a magnitude that it was impossible to determine the precise values of γ_o. Admittedly not enough evidence is given here to completely eliminate the possibility of mechanical irregularity at the orifice introducing the effect or the possibility of some weird hydrodynamical effect taking place.

Nevertheless, it is informative to speculate with the data available. The following model is proposed to explain the phenomena observed. Let the surface at time t be composed of two types of water molecules which make up a monolayer. Type 1 has the configuration characteristic of the bulk. Type 2 has the configuration of the equilibrium surface. The proposal of considering the surface as a special two dimensional monolayer cannot be too incorrect. McBain, Bacon and Bruce (30b) measured retardation in phase sustained by plane polarized light at a transparent reflecting surface to determine the depth of the surface layer. Their experiments implied the depth to be 2-3 Å. deep.

Before the fresh surface is formed, all of the water molecules in the monolayer have the configuration of type 1. For $t > 0$ the molecules of type 1 are converted to molecules

of type 2 at a measurable rate. At infinite time all of the molecules are of type 2. Assuming that the molecules of type 1 and type 2 form an ideal mixture, the surface tension at time t, $\gamma_{(t)}$, is given by the equation

$$\gamma_{(t)} = \gamma_o X_o^{\sigma}\ (t) + \gamma_\infty\ X_\infty^{\sigma}\ (t) \qquad (18)$$

where γ_o and γ_∞ have the same meaning as given by Schmidt and Steyer (44). $X_o^{\sigma}(t)$ is the surface mole fraction of molecules of type 1 (i.e., $X_o^{\sigma}\ (t) = \frac{\Gamma_2(t)}{\Gamma_1(t) + \Gamma_2(t)}$). Substituting equation 18 into equation 17, noting $X_\infty^{\sigma} + X_o^{\sigma} = 1$ and taking the derivative with respect to t one obtains

$$\frac{dX^{\sigma}}{dt^{o}} = -\alpha X_o^{\sigma} \qquad (19)$$

Thus one may treat the problem of reorientation as a first order kinetics problem. It is supposed that the type 1 molecules are undergoing a rearrangement to molecules of type 2. By making an Arrhenius plot of $\ln \alpha$ versus 1/T the energy of activation of the rearrangement is obtained. Figure 19a is such a plot. The energy of activation for the reorientation was found to be 9.9 K cal. This is in good agreement with the proposed model. In order for molecules of type 1 to reorient, it is necessary for one or more hydrogen bonds to be broken. The energy of a hydrogen bond is of the order of 6 K cal. (33).

The integrated form of equation 19 is

$$X_o^{\sigma} = \exp(-\alpha t) \qquad (20)$$

By definition the relaxation time is the time τ for fraction 1/e of the molecules of type 1 to have assumed orientation of type 2. Hence the relaxation time τ is equal to $1/\alpha$. The values of α corresponding to the temperature at 20°C. and 0°C. were taken from Figure 20a and the calculated relaxation times were found to be 3.5×10^{-3} and 1.2×10^{-2} seconds respectively.

A correction curve for the dynamic surface tension of water was obtained by finding α at 20°C. from Figure 20a and then using equation 17 calculate a $\gamma_{(t)}$ versus t curve. This was used in part C. above.

E. Theory

The problem of adsorption at the solution-air interface controlled by the kinetics of entry into the surface may be formulated in terms of the absolute reaction rate theory (21). The basic assumption is that reactant molecules (these may be both bulk molecules and surface molecules) are in equilibrium with an activated complex whose decomposition yields a molecule, or molecules, in the surface. Let B denote the molecules in bulk and S the molecules in the surface. The reaction may be

expressed by the general equation

$$mB + nS \rightleftharpoons (B_mS_n)^{\ddagger} \xrightarrow{k_1} (m-r)B + (n+r)S \qquad (21)$$

According to the absolute reaction rate theory the rate at which the activated complex decomposes is proportional to the concentration of the activated complex, i.e.,

$$k_1 = \frac{kTC}{h} (B_mS_n)^{\ddagger} \qquad (22)$$

where $C_{(B_mS_n)^{\ddagger}}$ is the concentration of the activated complex and kT/h is a universal rate constant which has the dimensions seconds^{-1}, and represents the frequency with which the activated complex decomposes to yield the adsorbed molecules. At 300°C. kT/h has a value of 5×10^{-12} sec.$^{-1}$.

The equilibrium between the reactants and the activated complex may be expressed by the equation

$$K = \frac{a^{\ddagger}}{a_B^{\,m}\, a_S^{\,n}} = \frac{C_{(AmSn)^{\ddagger}}\, \gamma^{\ddagger}}{a_A^{\,m}\, a_S^{\,n}} \qquad (23)$$

where $a^{\ddagger}$ is the activity of the activated complex, a_B is the activity of the adsorbate molecules in the bulk solution, a_S is the activity of the adsorbate molecules in the surface, and $\gamma^{\ddagger}$ is the activity coefficient of the activated complex.

The rate at which the surface concentration, Γ moles/cm.^{2}, increases may be obtained by combining equation 23 and equation

Figure 19a. Arrhenius plot of data for water

Figure 19b. Dependence of K_D on chain length

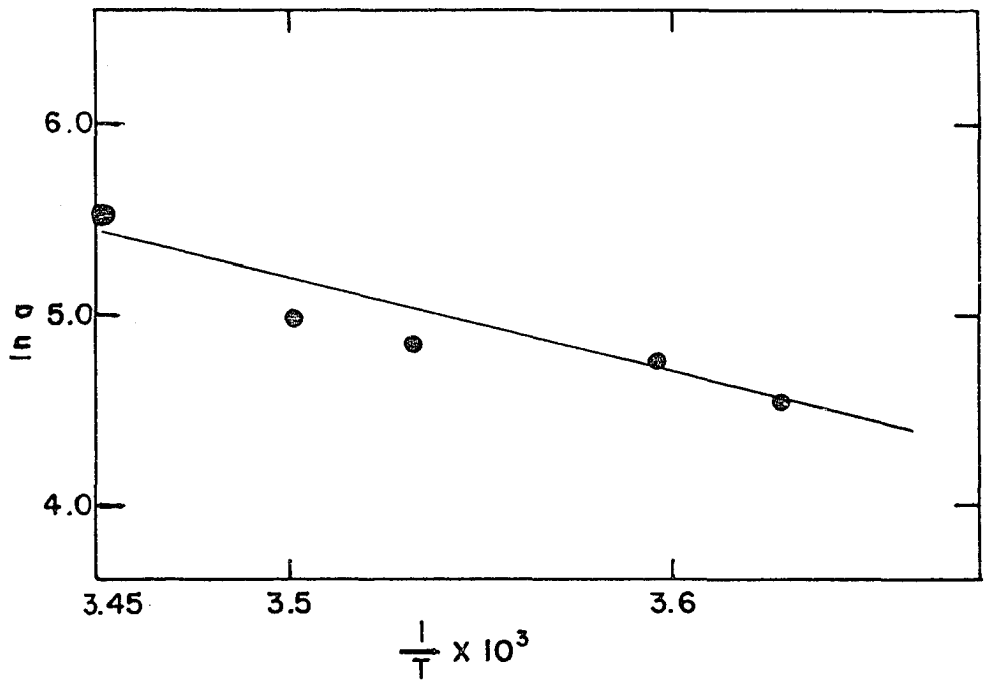
6.0
5.0
4.0
ln α
3.45
3.5
3.6
1/T X 10³

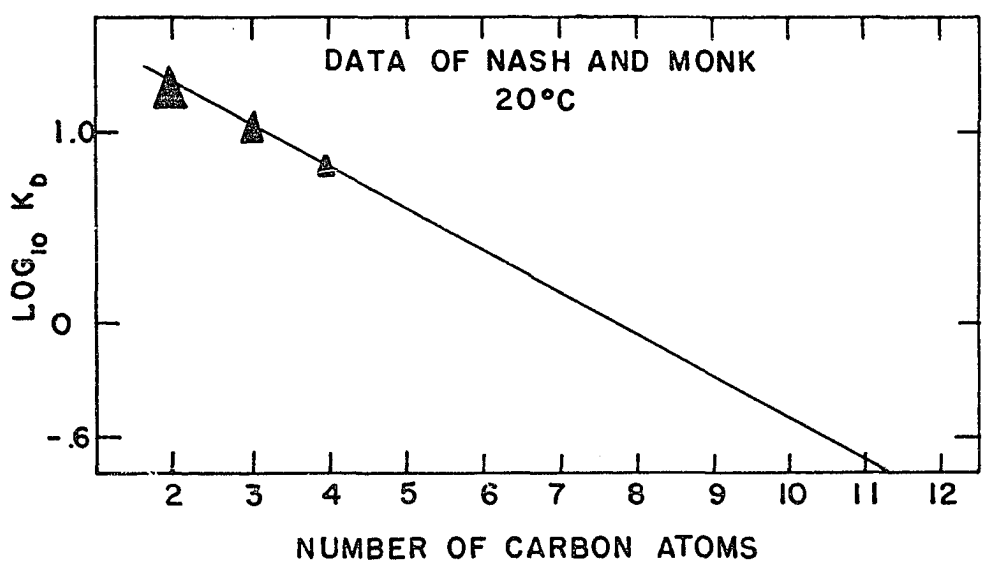
DATA OF NASH AND MONK
20°C
1.0
0
-.6
LOG10 Kb
2
3
4
5
6
7
8
9
10
11
12
NUMBER OF CARBON ATOMS

22.

$$\frac{d\Gamma}{dt} = \alpha \frac{kT}{h} K \frac{a_B^m a_S^n}{\gamma^{\ddagger}} = K_1 \frac{a_B^m a_S^n}{\gamma^{\ddagger}} \qquad (24)$$

where α is a proportionality constant. Here, a_S and $\gamma^{\ddagger}$ are functions of time. a_B remains effectively constant.

By the principle of microscopic reversibility (i.e., the reverse of the forward reaction must go through the same activated complex as the forward reaction) the net rate at which molecules are adsorbed into the surface may be expressed as

$$\frac{d\Gamma}{dt} = K_1 \frac{a_B^m a_S^n}{\gamma^{\ddagger}} - K_2 \frac{a_B^{m-k} a_S^{n+k}}{\gamma^{\ddagger}} \qquad (25)$$

At equilibrium it must be true that

$$K_{equil.} = \frac{K_1}{K_2} = \frac{a_S^k}{a_B^k}$$

Further it is required that at equilibrium the chemical potential in the bulk solution be equal to the chemical potential in the surface, hence $a_S = a_B$ if the same standard state is taken for bulk and surface materials. From this it is clear that $K_1 = K_2$ and that equation 25 may be rearranged to yield

$$\frac{d\Gamma}{dt} = \frac{\beta}{\gamma^{\ddagger}} (a_B^m a_S^n - a_B^{m-k} a_S^{n+k}) \qquad (26)$$

If the experimentally determined values of m, n and k are introduced at this point, the following formulation is simplified. From the experimental data it was found that m = 2, n = 0 and k = 1. Hence equation 26 becomes

$$\frac{d\Gamma}{dt} = \frac{\beta}{\gamma\ddagger}(a_B^2 - a_B a_S) \qquad (27)$$

It is now necessary to define the reference states to which the various activities are referred. In this work the concentration in bulk will be referred to as C_B. It is defined by the relation $C_B = C_T - C_{B^-} - C_S \approx C_T - C_{B^-}$, where C_T is the total concentration C_{B^-} is the concentration of the ionized fatty acid and C_S is the concentration of the fatty acid on the surface, all in moles per liter solution (M/ls). Since $C_S \ll C_{B^-}$ it is neglected. From this it is clear that $a_B + C_B\gamma_B$, where γ_B is the activity coefficient of the adsorbate molecules in the bulk. Since all of the concentrations used here are less than .01 molar, it is assumed the adsorbate in bulk follows Henry's law. The standard state for the adsorbate in bulk is defined as infinite dilution, i.e.,

$$\lim_{C_B \to 0} a_B/C_B = 1$$

Further, over the concentration range used here it is assumed that a_B may be replaced with C_B.

It is more convenient to talk about the activity of the surface molecules in terms of fugacities. By definition $a_S = f_S/f_S^{\circ}$, where f_S is the fugacity in the surface and f_S° is a reference fugacity to be defined. The surface fugacity is related to the spreading pressure by the equation

$$RT\ln (f_S/\pi) = \int_0^{\pi} (\bar{A} - RT/\pi')d\pi' = RT\ln\gamma_S \qquad (28)$$

where π is the spreading pressure, $\bar{A}$ is the area per mole of the adsorbed molecule and γ_S is the activity coefficient in the surface. From the requirement, $a_B = a_S$, at equilibrium one gets the relation

$$a_B = C_B = f_S/f_S^{\circ} = \frac{\pi}{f_S^{\circ}}\left[\exp\left\{\int_0^{\pi} \left(\frac{\pi'\bar{A}/RT - 1}{\pi'}\right)d\pi'\right\}\right] \qquad (29)$$

It is necessary to choose a reference fugacity based on infinite dilution in the film. Thus as $\pi \rightarrow 0$, $\exp\left\{\int_0^{\pi} \left(\frac{\pi'\bar{A}/RT - 1}{\pi'}\right)d\pi'\right\} \rightarrow 1$, $\gamma_S \rightarrow 1$ and $C_B \rightarrow 0$. Thus one may rearrange equation 29 to yield

$$f_S^{\circ} = \lim_{\substack{\pi \rightarrow 0 \\ C_B \rightarrow 0}} \pi/C_B$$

From this definition it is clear that the reference fugacity is equal to Traube's constant, f_o (33).

Further it should be noted that at equilibrium

$$C_B = a_B = a_S\ (t = \infty) = f_S\ (t = \infty)/f^o$$

Equation 27 may now be written as

$$\frac{d\Gamma}{dt} = \frac{\beta\, C_B}{\gamma^{\ddagger} f_o^{\,o}} \left[f_S\ (t = \infty) - f_S(t) \right] \longrightarrow \frac{\beta\, C_B}{\gamma^{\ddagger} f_o} \left[f_S\ (t = \infty) - f_S(t) \right] = \frac{\beta\, C_B}{\gamma^{\ddagger} f_o^{\,o}} \left[\pi_\infty \exp \int_0^{\pi_\infty} \left(\frac{\pi' \bar{A}/RT - 1}{\pi'} \right) d\pi' - \pi \exp \int_0^{\pi} \left(\frac{\pi' \bar{A}/RT - 1}{\pi'} \right) d\pi' \right]$$

$$= \frac{\beta\, C_B}{\gamma^{\ddagger} f^o} \frac{\gamma_S}{\gamma^{\ddagger}} \left[\pi_\infty \exp \int_{\pi}^{\pi_\infty} \left(\frac{\pi' \bar{A}/RT - 1}{\pi'} \right) d\pi' - \pi \right] \qquad (30)$$

where π is a function of time.

The rate constant β may now be determined if the corresponding values of $d\Gamma/dt$ for a given π (t) is known and if the integral $\int_{\pi}^{\pi_\infty} \left(\frac{\pi' \bar{A}/RT - 1}{\pi'} \right) d\pi'$ can be evaluated. $d\Gamma/dt$ may be evaluated from equation 16. Taking the derivative of equation 16 after π one obtains

$$\frac{d\pi}{dt} = k\, \pi_\infty^{\,3} F(u) \qquad (31)$$

where $F(u) = \frac{(1-u)^2 \exp(bu)}{1-bu\,(1-u)}$ and $u = \pi/\pi_\infty$.

It is convenient at this point to introduce the relation $\phi = \pi\bar{A}/RT - 1$. Then noting that $\bar{A} = 1/\Gamma$ and that

$\Gamma = \pi/RT\ (1 + \phi)$ one may obtain

$$\frac{d\pi}{dt} = \frac{1}{RT(1+\phi)^2}\left(1 + \phi - \pi \frac{d\phi}{d\pi}\right)\frac{d\Gamma}{dt} = k\,\pi_{\infty}^{3}F(u). \quad (32)$$

where $d\Gamma/dt$ is given by equation 30. The evaluation of the integral $\int_{\pi}^{\pi_{\infty}} (\phi/\pi')\,d\pi'$ can be obtained with the aid of equation of state data.

Schofield and Rideal (45, 46) have studied soluble surface films and have found that they can represent their data by equation of state of the form

$$\frac{\pi\bar{A}}{RT} = \frac{\pi B}{RT} + x \quad (33)$$

for $\pi > 8$ dyne/cm. B is a constant and is identified as the minimum area per mole that an adsorbate at the solution-air interface can occupy. 1/x is a measure of the relative cohesive energy between the molecules. Figure 20 is a plot of $\pi\bar{A}/RT$ versus π[1]. For $\pi > 8$ dyne/cm., the slopes of the curves representing the four fatty acids are constant and equal. The value of the slope is B/RT, hence the limiting area is of the order of 24-25 Å^2.

At π very near 0 the value of $\pi\bar{A}/RT$ is very nearly 1.

---

[1]The method used to calculate the results for the heptanoic acid and hendecanoic from π, c data was that used by Schofield and Rideal (45). The octanoic and decanoic curves are from the data given by them corrected to 20°C.

This implies that the molecules in the surface act as an ideal two dimensional gas. As π is increased there is a sharp decrease in the value of $\pi \bar{A}/RT$. This corresponds to the mutual attraction between the molecules. The fact that the decrease of $\pi \bar{A}/RT$ is greater the longer the fatty acid indicatesthat the lateral attraction between the hydrocarbon tails is predominant. Near the minimum of each curve the attractive force is compensated by the incompressibility of the molecules (size effect) and possibly dipole-dipole repulsion. Past the minimum these replusive effects counteract the attractive forces to give the linear relation. This may be somewhat fortuitous, but as noted before this limiting slope is taken as a measure of the cross-sectional area.

In the evaluation of the rate constant β, the deviation of the equation of state from the experimental data was taken into account by not using values of π corresponding to the non-linear section of the curve. It should be noted that even over the linear portion of the equation of state curves the scatter of the experimental data is fairly great, but there isn't any other satisfactory relation to use. Finally, from the great deviation of the curves from a horizontal straight line (i.e., $\pi \bar{A}/RT = 1$) it is to be expected that γ_S will vary greatly.

Introducting equation 33 into equation 30 and equation 32 it is found that the product of the rate constant and the ratio of the activity coefficients may be expressed as

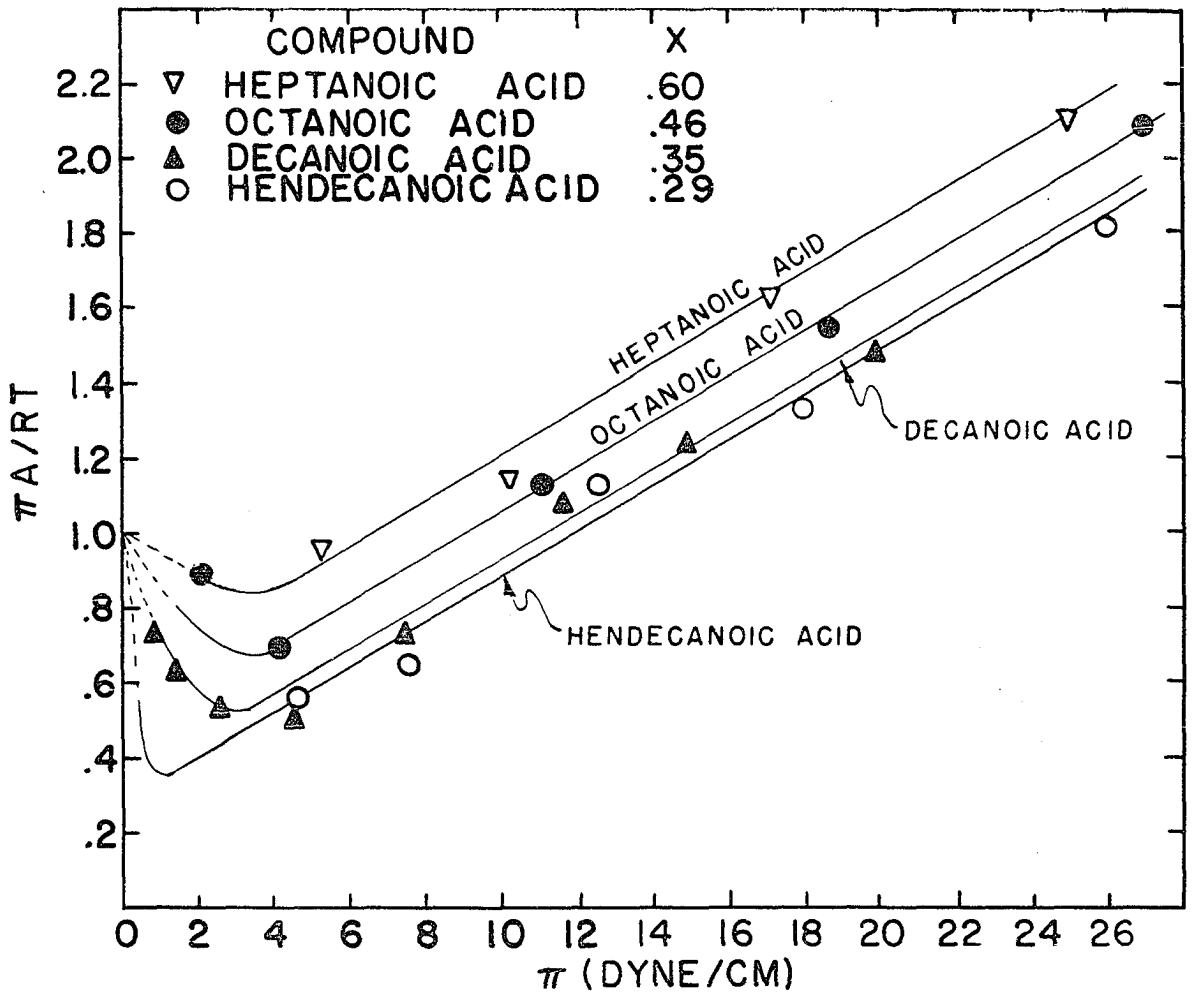

Figure 20. Dependence of $\pi A/RT$ on π

$$\beta \frac{\gamma_s}{\gamma^{\ddagger}} = \frac{x f_o k \pi_\infty^3 F(u)}{RTC_B(x+\frac{B\pi}{RT})^2\left\{\pi_\infty(\frac{\pi_\infty}{\pi})^{x-1}\exp -B(\frac{\pi_\infty-\pi}{}) - \pi\right\}}$$

$$= G(\pi) \qquad (34)$$

The assumption is made that the ratio of the activity coefficients depends only on π regardless of the concentration. Consequently the rate constant β may be found by taking the limit

$$\lim_{\pi \to 0} G(\pi) = \beta \qquad (35)$$

Figure 21 is a plot of $G(\pi)$ versus π. It is seen that the assumption that $\gamma_s/\gamma^{\ddagger}$ is independent of the concentration is correct. It becomes apparent that the definition of the standards states has reduced the representation of the data for all of the fatty acids studied to one equation with only one rate constant, β.

It is apparent that it would be impossible to extrapolate the curve to $\pi = 0$ in Figure 22, consequently a plot of $\log_{10} G(\pi)$ versus π was made and the value of β determined. See Figure 22. The value of β determined from Figure 23 is $.8 \pm .3$ liter^2/moles-sec.-cm.^{2}.

The interpretation of the kinetic mechanism as revealed by equation 27 leads to the following conclusions. The rate of adsorption is second order in the bulk concentration. Due

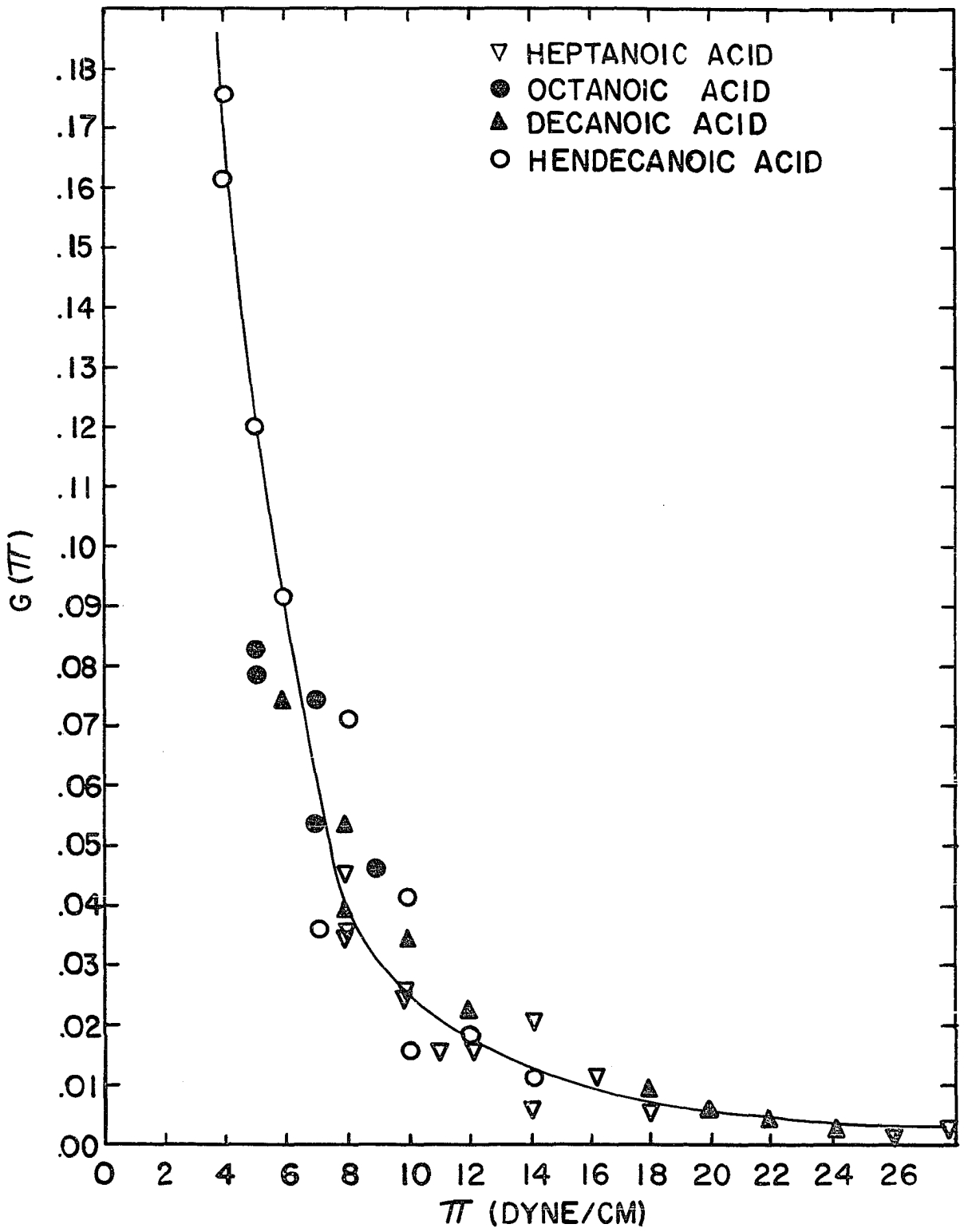

Figure 21. Dependence of G(π) on π

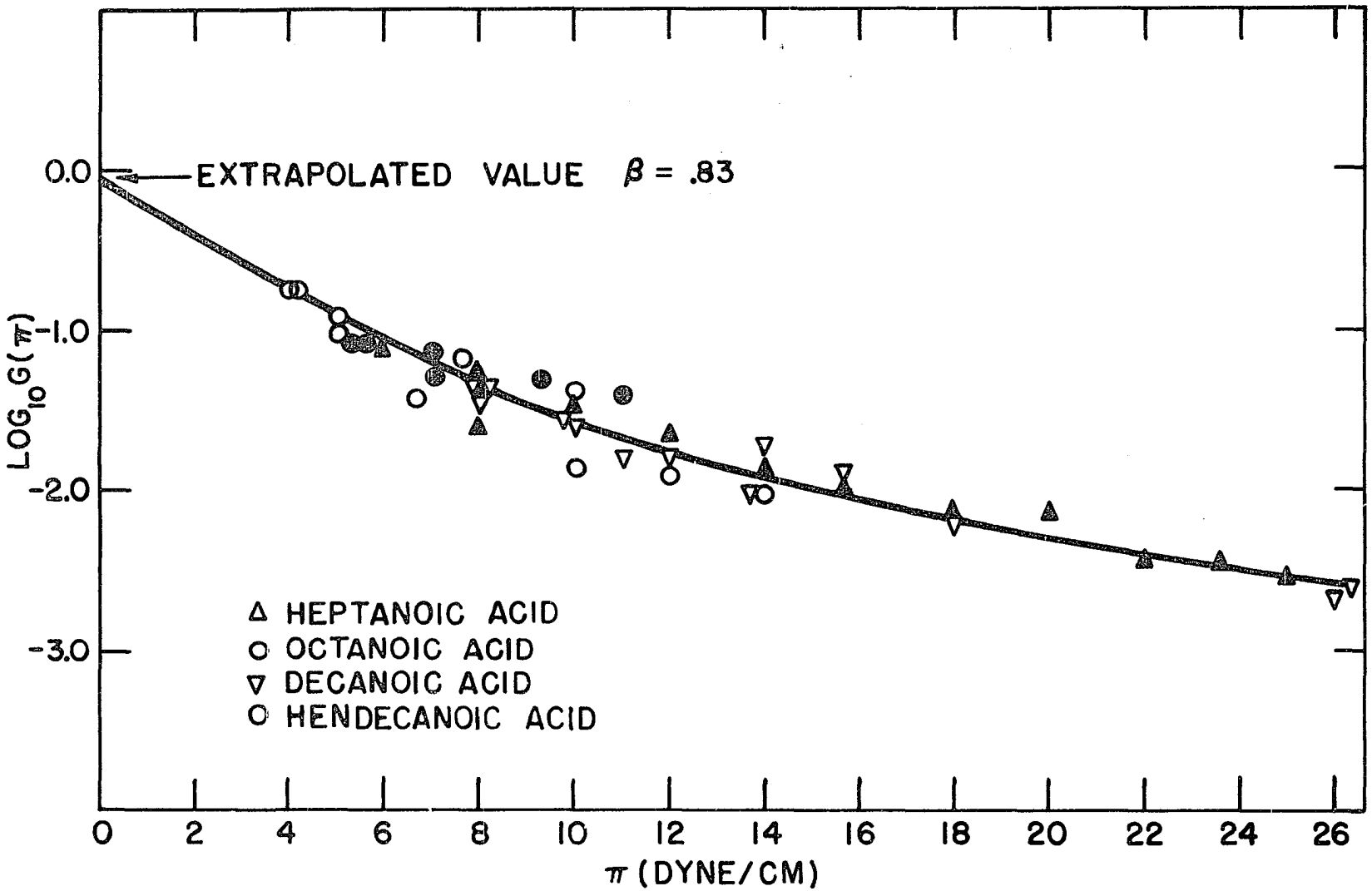

Figure 22. Extrapolation of the rate constant β

to the fact that the bulk concentration does not change perceptably over a run, the rate of adsorption is constant for a given concentration. The independence of the rate of adsorption explicitly on the surface concentration is characteristic of a mobile monolayer as one must certainly have in the case of soluble surface films.

The rate of desorption is more complicated to interpret. The desorption is first order in bulk concentration and first order in surface activity. Since it is easier to think in terms of concentration it is useful to replace the surface activity by a series of approximation. In the initial part of the adsorption $a_S = f_S/f_o \lesssim \pi/f_o \cong \alpha\Gamma/f^o$. Hence the initial desorption may be represented by

$$\frac{\overleftarrow{d\Gamma}}{dt} = \frac{K' C_B \Gamma}{f^o}$$

K' should be constant for the series of acids studied in this work. The constant $K'' = K'/f^o$ will decrease by a constant factor for each additional CH_2 group added to the fatty acid. This is the well known ratio 3.5.

The results obtained here may be compared qualitatively with the results obtained by Posner and Alexander for aqueous solutions of hexanol, heptanol and octanol. They based their representation on a Langmuir type kinetic equation (see equation 8). Converting their symbology to that used here, their rate of adsorption (see equation 8) is given by

$d\Gamma/dt = k_1 C_B (\Gamma_S - \Gamma)$, where Γ_S is the saturated surface concentration in moles/cm.^{2}. They found that k_1 was constant for all three alcohols. This would correspond to the constancy of β in the corresponding adsorption equation. They found that the desorption was given by $d\Gamma/dt = K'_2\Gamma$. Here K' decreased by a factor 1.7 in going from hexanol to heptanol and 2.4 in going from heptanol to octanol. Again the trend is the same as that found here (i.e., decreases by a factor of 3.5 for each additional CH_2).

The second order dependence on bulk concentration implies some sort of interaction between two bulk molecules. The most probable way for the two bulk molecules to form the transition state is through hydrogen bonding to form dimers.

Nash and Monk (32) have recently determined the dimerization constant, K_D, for acetic, propionic and butryic acids in water by e.m.f. measurements. The dimerization constant they found represented the reaction $A_2 \rightleftharpoons 2A$, where A_2 is the dimer and A is the monomer. In order to determine the range of the dimerization constants of the fatty acids used in this work, a plot of $\log_{10} K_D$ versus the number of carbon atoms in the fatty acid molecule was made (see Figure 19b). The relation between the three points determined by Nash and Monk is fairly linear and should yield good approximations. It was found that K_D varied from 1.2 for heptanoic acid to about 1/3 for hendecanoic acid. The fact that the dimerization constant in water can be measured for fatty acids is support for the existence of the transition state as a dimer.

Further, it is possible to make an independent approximate calculation of β. The second order dependence may be interpreted to mean that the initial rate at which the bulk molecules are adsorbed is dependent upon the concentration of dimers within a characteristic distance of the surface, τ, (in arguments of this kind (21) it is usual to assume that is of the order of a molecular diameter). Therefore

$$\left(\frac{d\Gamma}{dt}\right)_{initial} = \frac{C_D \tau \nu}{} = \frac{C_B^2 \tau \nu}{K_D} = \frac{C_B^2 \tau \nu}{10^3 K_D} \text{ (moles/cm.}^2\text{-sec.)},$$

where C_D is the concentration of the dimer in moles per liter and ν is the characteristic frequency of the absolute reaction rate theory (21). At 20°C. ν is about 4×10^{12} sec.$^{-1}$. The factor 10^3 is needed in the above equation to convert moles/liter to moles/cm.^{3}. The initial rate of adsorption according to equation 27 is $\left(\frac{d\Gamma}{dt}\right)_{initial} = \beta C_B^2$ (moles/cm.^{2}-sec.). Hence

$$\beta = \frac{\tau \nu}{10^3 K_D} = \frac{10^{-8} \times 4 \times 10^{12}}{10^3 \times 1} \approx 40 \qquad (36)$$

The agreement with the determined value of $\beta \approx 1$ is fairly good. One would expect the value of β determined by this simple model to be larger than that found experimentally, because the model assumes molecules of all orientations will enter the surface, whereas it is more likely that only molecules of certain orientations can enter.

One more bit of information may be inferred about the transition state; namely, its effective cross-sectional area. If the natural logarithm is taken of both sides of equation 34 the following result is obtained:

$$\ln \gamma - \ln \gamma^{\ddagger} = \ln G(\pi) - \ln \beta \qquad (37)$$

From equation 27

$$\ln \gamma = \int_0^{\pi} \frac{\phi}{\pi'} \, d\pi'$$

it is clear that $\gamma^{\ddagger}$ can be calculated as a function of π only. The dependence of $\gamma_s / \gamma^{\ddagger}$ solely on π implies that the transition state is probably very near the final state along the reaction coordinate. The transition state will be interpreted to be film like in nature and $\ln \gamma^{\ddagger}$ will be defined as $\int_0^{\pi} \left(\frac{\pi' A^{\ddagger}/RT - 1}{\pi'} \right) d\pi'$. Further the transition state will have associated with it an equation of state and it will be assumed that it will be similar to that in the surface. Substituting for $\ln \gamma$ and $\ln \gamma^{\ddagger}$ into equation 37 and taking the derivative after π one obtains

$$\frac{\phi - \left(\frac{\pi A^{\ddagger}}{RT} - 1 \right)}{\pi} = \frac{d \ln G(\pi)}{d\pi} = \frac{\pi \bar{A} - \pi \bar{A}^{\ddagger}}{RT} \qquad (38)$$

Then recalling that the equation of state of the surface film was of the form $\pi \bar{A}/RT = \pi B/RT + x$, equation 38 may be

rearranged to yield

$$\frac{B - B^{\ddagger}}{RT} + \frac{x - x}{\pi} = \frac{d\ln G(\pi)}{d\pi} \qquad (39)$$

where B is the limiting area of the molecule in the surface, $B^{\ddagger}$ is identified as the limiting area of the transition state, x and $x^{\ddagger}$ are measures of the relative cohesive forces in the film and transition state respectively. In the limit as π becomes large

$$\frac{B^{\ddagger} - B}{RT} = \frac{-d\ln G(\pi)}{d\pi} \qquad (40)$$

From Figure 22 it is seen that for $\pi > 20$ dyne/cm. that $-d\ln G(\pi)/d\pi$ is essentially constant. The contribution of $\frac{(x - x^{\ddagger})}{20}$ would be less than .03; hence the limiting value of the slope is found to be 0.108. The value of B/RT found from Figure 21 is 0.060. Thus it would appear that the effective limiting area of the transition state molecule is approximately 2 3/4 time as large as the limiting area of a single molecule in the surface. This result is in accord with the proposed dimer model.

Soluble layers of surface films have associated with them a surface potential (16, p. 68). The surface potential is the difference in potential of the water surface and the adsorbed layer. This implies that the adsorbed molecules at the surface have a preferential orientation. This orientation gives rise

to an electrical double layer. It is apparent that it would cost less energetically to move a molecule into the surface through the field of the double layer if the dipole of the molecule was effectively canceled. The net dipole moment of a dimer should be effectively zero. There is some evidence that there is a double layer at the surface of pure water. Frenkel (19) has pointed out that the surface layer of any pure liquid could be considered as a monomolecular film adsorbed on the surface of that same liquid. If the dipoles only are considered the surface could take two equally advantageous orientations corresponding to inward and outward moments. If, however, the quadropole moment is also taken into account, one of these orientations must be more advantageous than the other.

Verwey (54) has given evidence that the above postulate of Frenkel's is essentially true. The absolute magnitude of the potential at the surface of water is impossible to measure, but to the same extent that chemical potential of individual ions may be estimated, the potential at the surface of water can also be estimated. He calculated the potential at the water-vacuum interface from the work functions for Na , K and Ag ions and the free energy of hydration determined by the interaction of the ions with their immediate surroundings. He concluded water is about $\frac{1}{2}$ volt more negative than the vacuum and that consequently the protons of the water molecules in the surface layer are oriented toward the surface. He has shown that this is in agreement with the ice-like structure of liquid

water.

An exact calculation of the energy required to move a dipole through a dipole field would prove to be quite complex. An approximate estimate can be made by assuming that the energy required would be of the order of rotating a dipole through 180° in the field. An electronic charge situated in an electrical field of strength E is acted upon by a force of magnitude eE, in the direction of the electric field. The magnitude of a couple (i.e., dipole) in the field is $deE \sin\Theta$, where Θ is the angle the axes of the couple makes with the direction of the field and d is the distance between the charges. Consequently the work in turning the couple from where it is parallel to the field through 180° is

$$W = \int_0^{180} deE \sin\Theta \, d\Theta = 2deE = 2\mu E.$$

Taking the potential across a double layer to be of the order of 1 volt, the distance across the field 1×10^{-8} cm., and $\mu \approx 2\times10^{-18} = (e/3)\ 1.3\times10^{-8}$ (Debyes) one finds that W is of the order of 7.2 K cal/mole. 7.2 is not an unreasonable value and would definitely indicate that energetically it would be less costly to move the molecules into the surface dimerized.

F. Proposed Future Work

The variation of β with temperature still needs to be worked out. Not enough information was obtained with the heptanoic acid at 10°C. to be helpful. The information would

yield the magnitude of the activation of energy. The value of this would give a clearer picture of the nature of the energy barrier to entry.

This same treatment applied to other homologous series such as the aliphatic alcohols would be of value in the study of the effect of constituent groups on the rate and mechanisms of adsorption.

A more direct method is needed to verify the apparent reorientation that was found to take place at a freshly formed water surface. If a reorientation is actually taking place, it is to be expected that the vertical component of the dipole moment and hence the potential of the surface of the water molecules would change with time. It is impossible to measure the absolute magnitude of the potential, but the change in potential can be measured. Various schemes have been devised for this (26). An apparatus could be designed similar to that of Posner and Alexander (35) to study the change in surface potential along the jet of water. Since the reorientation appears to take place in the first 2 cm. or so of the jet, one should be able to record the surface potential as a function of distance from the orifice. This should either verify or refute the results given herein and might also lead to some information as to the actual structure of the surface layer.

The data obtainable from a mercury jet would be of great interest. In principle an experiment with a mercury jet could be performed with a modification of the experimental technique

used in this work. A reflection technique would have to be used in place of the transmission technique to measure the wave length. A section of the node on the mercury surface would form a parabolic section which would reflect and focus the parallel illuminating light at a point. Whether the surface of the node would be of sufficient area to give measurable spots would have to be determined. The kinetics of adsorption at the mercury-vapor interface could be studied. A mercury jet could be discharged into a cell with a vapor (i.e., such as hexane) at equilibrium with its liquid. The adsorbed vapor would change the surface tension which is measurable and hence the kinetics of the adsorption could be followed. Further, the mercury jet could be discharged through a solution and the kinetics of adsorption at the mercury-solution interface could be determined. It would also be interesting to see if any correlation could be found between the results obtained by this method and equilibrium adsorption measurements such as those of Hansen, Minturn and Hickson (24) at the solution-mercury interface.

VII. SUMMARY

1. Time and concentration dependence of the surface tensions of aqueous solutions of pentanoic, heptanoic and octanoic acids and heptanol-1 were determined at 20°C. Heptanoic acid solutions were also investigated at 10°C.

2. Incident to this study, the vibrating jet method for measuring surface tensions of nearly new surfaces was studied; methods of calculating surface tensions and surface ages were fundamentally revised (this portion of the work was partially in collaboration with Dr. M. E. Purchase). It was discovered that flow properties of the issuing jet at the orifice were markedly improved by treating the orifice with a silicone.

3. It was found that the empirical relation

$$\frac{u}{1-u} = k\,\pi_\infty^2\, e^{bu}t \qquad (1)$$

in which $u = \frac{\pi}{\pi_\infty}$, π_∞ is the equilibrium spreading pressure, π the spreading pressure at time t, and k and b are constants, represented the dependence of spreading pressure (surface tension of solvent minus surface tension of solution) on concentration and time to an excellent degree of approximation. This same equation was found to represent data of Addison for aqueous solutions of decanoic acid, and of Dervichian for aqueous solutions of hendecanoic acid.

4. The constant b in equation 1 was found to be nearly

independent of adsorbate, and the constant k was found to vary uniformly with adsorbate chain length over the series including both results from the present work obtained by the vibrating jet technique and results of Addison and Dervichian, obtained by conventional surface tension techniques. This furnishes strong evidence that the vibrating jet technique, coupled with the method of interpretation developed herein, yields objective results for the variation of surface tension with time.

5. No mechanisms could be found which provided a kinetic interpretation of equation 1. Therefore, alternate rate expressions were investigated in a search for one which would be approximately equivalent, in differential form, to equation 1 and which would be susceptible to kinetic interpretation. The following rate expression was found to represent adequately all available experimental data:

$$\frac{d\Gamma}{dt} = \frac{\beta C_B}{\gamma^{\ddagger}} (C_B - a_S) \qquad (2)$$

in which Γ is the adsorbate surface excess at time t, C_B is the adsorbate concentration, a_S is the adsorbate activity in the adsorbed film at time t (referred to a standard state such that the activity coefficient is unity at infinite dilution in bulk solution) and $\gamma^{\ddagger}$ is the activity coefficient of the activated complex at time t. Equation 2 was used with equation 1 to obtain the ratio $\gamma_S/\gamma^{\ddagger}$ where γ_S is the activity coefficient of adsorbate in the surface film at time t; it was

found that this ratio depended on π only and from this it may be concluded that the transition state occurs in or near the surface film. The constant β is found to be of the same order of magnitude not only for all substances studied in the present work, but also for the systems investigated by Addison and Dervichian by conventional surface tension techniques.

6. It is concluded that the adsorption of the normal aliphatic acids C_5 - C_{11} and of heptanol-1 can be treated by kinetic theory and adsorption mechanisms inferred similar to the manner used in the study of bulk reaction mechanisms, and that in all of the above cases the adsorption rate determining step is second order in adsorbate. Possible reasons for this order are discussed.

7. The possibility of a diffusion controlled adsorption rate process is examined and rejected. It is shown that an erroneous conclusion in this respect has apparently been reached by other workers exploiting the vibrating jet technique because they have incorrectly obtained their surface ages and the magnitude of their error is sufficient to account for an initially linear variation of surface pressure with time appear to be a linear variation with the square root of time.

8. An apparently significant variation of the surface tension of pure water with time as a function of temperature was found. A possible mechanism is suggested, and possible confirmatory experiments suggested.

VIII. LITERATURE CITED

1. Addison, C. C. J. Chem. Soc. 1943, 535.
2. _____ J. Chem. Soc. 1944, 252.
3. _____ J. Chem. Soc. 1944, 477.
4. _____ J. Chem. Soc. 1945, 98.
5. _____ J. Chem. Soc. 1946, 579.
6. Bohr, N. Trans. Roy. Soc. (London) A209, 281 (1909).
7. Bond, W. N. Proc. Phys. Soc. (London) A47, 549 (1935).
8. _____ and Puls, H. O. Phil. Mag. Seventh Ser. 24, 864 (1937).
9. Boutaric, A. and Berthier, P. J. chim. phys. 36, 1 (1939).
10. Brockman, M. R. J. Research Nat. Bur. Standards 58, 51 (1957).
11. Buchwald, E. and Konig, H. Ann. Physik 26, 659 (1936).
12. Burcik, E. J. J. Colloid Sci. 5, 421 (1950).
13. _____ J. Colloid Sci. 8, 520 (1953)
14. _____ and Newman, R. C. J. Colloid Sci. 9, 498 (1954).
15. _____ and Vaughn, C. P. J. Colloid Sci. 6, 522 (1951).
16. Butler, J. A. V. The Electrical Double Layer and Electrocapillarity. In J. A. V. Butler, ed. "Electrical Phenomena at Interfaces." pp. 30-74. London. Methuen and Co., Ltd. 1951.
17. Dervichian, D. G. Kolloid-Z. 146, 96 (1956).
18. Eggenberger, D. N., Broome, F. K., Ralston, A. W. and Harwood, H. J. J. Org. Chem. 14, 1108 (1948).
19. Frenkel, J. "Kinetic Theory of Liquids." New York. Dover Publications, Inc. 1955.

20. Frumkin, A. Z. physik. Chem. 116, 498 (1925).

21. Glasstone, S., Laidler, K. J. and Eyring, H. "The Theory of Rate Processes." New York. McGraw-Hill Book Co., Inc. 1941.

22. Goldstein, S. Proc. Cambridge Phil. Soc. 26, 1 (1930).

23. _____ Proc. Roy. Soc. (London) A142, 545 (1933).

24. Hansen, R. S., Minturn, R. E. and Hickson, D. A. J. Phys. Chem. 61, 953 (1953).

25. _____, Purchase, M. E., Wallace, T. C. and Woody, R. W. J. Phys. Chem. 62, 210 (1958).

26. Harkins, W. D. "The Physical Chemistry of Surface Films". New York. Reinhold Publishing Corp. 1952.

27. _____ and Brown, F. E. J. Am. Chem. Soc. 41, 499 (1919).

28. "International Critical Tables." Vol. 4. New York. McGraw-Hill Book Co., Inc. 1928.

29. King, H. H. Kans. State Agr. Coll., Tech. Bull. No. 9. 1922.

30a. Lund, H. and Bjerrum, J. Ber. deut. chem. Ges. 94, 149 (1920).

30b. McBain, J. W., Bacon, R. C. and Bruce, H. D. J. Chem. Phys. 7, 818 (1939).

31. Murphy, G. "Similitude in Engineering." New York. The Ronald Press Co. 1950.

32. Nash, G. R. and Monk, C. B. J. Chem. Soc. 1957, 4274.

33. Partington, J. R. The Properties of Liquids. In "An Advanced Treatise on Physical Chemistry." Vol. 2, pp. 174-192. New York. Longmans Green and Co. 1951.

34. Pedersen, P. O. Trans. Roy. Soc. (London) A207, 341 (1907).

35. Posner, A. M. and Alexander, A. E. Trans. Faraday Soc. 45, 651 (1949).

36. _____ and Alexander, A. E. J. Colloid Sci. 8, 575 (1953).

37. _____, Anderson, J. R. and Alexander, A. E. J. Colloid Sci. 7, 623 (1952).

38. Purchase, M. E. Dynamic surface tension measurements and their use in prediction of wetting ability. Unpublished Ph.D. Thesis. Ames, Iowa, Iowa State College Library. 1957.

39. Ralston, A. W. and Hoerr, C. W. J. Org. Chem. 7, 546 (1942).

40. Rayleigh, Lord Proc. Roy. Soc. (London) A29, 71 (1879).

41. Rideal, E. K. and Sutherland, K. L. Trans. Faraday Soc. 48, 1109 (1952).

42. Ross, S. and Haak, R. M. J. Phys. Chem. (ca. Oct. 1958).

43. Schiller, L. Forscharb. Gebiete Ingenieurw. 248, 1 (1922).

44. Schmidt, F. and Steyer, H. Ann. Physik 76, 442 (1926).

45. Schofield, R. K. and Rideal, E. K. Proc. Roy. Soc. (London) A109, 57 (1925).

46. _____ and _____ Proc. Roy. Soc. (London) A110, 167 (1926).

47. Smyth, C. S. "Dielectric Behavior and Structure." New York. McGraw-Hill Book Co., Inc. 1955.

48. Stocker, H. Z. physik. Chem. 94, 149 (1920).

49. Sutherland, K. L. Australian J. Sci. Research Ser. A. 5, 683 (1952).

50. _____ Australian J. Chem. 7, 319 (1954).

51. Ward, A. F. H. and Tordai, L. Nature 154, 146 (1944).

52. _____ and _____ J. Chem. Phys. 14, 453 (1946).

53. Weber, L. I. and Sternganz, P. Z. physik. Chem. 169, 241 (1934).

54. Verwey, E. J. W. Rec. trav. chim. 71, 572 (1952).

IX. ACKNOWLEDGMENT

The author wishes to express his sincere appreciation to Dr. Robert S. Hansen for his encouragement, suggestions and direction in this research. His enthusiasm and unique insight will not be forgotten.

The author would also like to express his thanks to his wife for her encouragement and sacrifice which have made the attainment of this goal possible.